Universidade de Aveiro
2020

Departamento de Eletrónica,
Telecomunicações e Informática

**Manar**
**Miri**

# Equalizador Hibrido na banda das ondas milimétricas para Sistemas GFDM

# Hybrid Equalizer for millimeter wave GFDM Systems

**Universidade de Aveiro**
**2020**

Departamento de Eletrónica,
Telecomunicações e Informática

**Manar**
**Miri**

# Equalizador Hibrido na banda das ondas milimétricas para Sistemas GFDM

# Hybrid Equalizer for millimeter wave GFDM Systems

Dissertação apresentada à Universidade de Aveiro para cumprimento dos requisitos necessários à obtenção do grau de Mestre em Engenharia Electrónica e Telecomunicações, realizada sob a orientação científica do Doutor Professor Adão Silva, Professor Auxiliar da Universidade de Aveiro do Departamento de Eletrónica, Telecomunicações e Informática da Universidade de Aveiro, e do Doutor Daniel Castanheira, investigador auxiliar no Instituto de Telecomunicações pólo de Aveiro.

.

This work is supported by the European Regional Development Fund (FEDER), through the Competitiveness and Internationalization Operational Program (COMPETE 2020) of the Portugal 2020 framework, Regional OP Centro (CENTRO 2020), Regional OP Lisboa (LISBOA 14-20) and by FCT/MEC through national funds, under Project MASSIVE5G (AAC no 02/SAICT/2017)

Global Platform for Syrian Students Scholarship.

**o júri / the jury**

presidente / president

Professor Doutor Armando Carlos Domingues da Rocha
Professor Auxiliar, Universidade de Aveiro

vogais / examiners committee

Professor Doutor Paulo Jorge Coelho Marques
Professor Adjunto, Instituto Politécnico de Castelo Branco

Professor Doutor Adão Paulo Soares da Silva
Professor Auxiliar, Universidade de Aveiro

**agradecimentos** /
**acknowledgements**

First of all, I would like to thank my supervisor Professor Adão Silva and my co-supervisor Doctor Daniel Castanheira for their continuous support, help, exceptional supervision, mentoring, and review of my thesis document with their expert opinions.

I would like to thank the Global Platform for Syrian Students represented by former President Jorge Sampaio and his Diplomatic Adviser Dr. Helena Barroco. I am very grateful for this great opportunity they gave to me as a first and significant step towards achieving my goals and making my dreams come true.

Last but not least, thank you very much to the University of Aveiro, the Department of Electronics, Telecommunications, and Informatics and the Instituto de Telecomunicações for providing the necessary conditions of work and learning.

**Palavras Chave**

5G,GFDM, terminais com número elevado de antenas, comunicações na banda das ondas milimétricas, arquiteturas híbridas analógico-digitais

**Resumo**

O uso de um número elevado de antenas, também designado por MIMO massivo, tem sido considerada uma das tecnologias mais promissoras para os futuros sistemas de comunicação sem fios. Esta tecnologia, refere-se à ideia de equipar as estações base (BSs) com um número muito grande de antenas, dando a possibilidade de focar a energia do sinal transmitido em áreas de alcance muito restritas, o que proporcionará grandes melhorias na capacidade, além das espectrais e eficiência energética. Simultaneamente, a exigência por taxas de dados elevadas e capacidade levou à necessidade de explorar uma enorme quantidade de espectro nas bandas de ondas milimétricas (mmWave). A combinação de comunicação na banda das ondas milimétricas com terminais equipados com um grande número de antenas tem o potencial de melhorar drasticamente os recursos da comunicação sem fios. Considerando no entanto uma arquitetura digital, usada em sistemas MIMO convencionais, em que cada cadeia de RF é dedicada a uma antena, implica um custo e um consumo de energia elevados. A solução é o uso de uma arquitetura híbrida, na qual um pequeno número de cadeias de RF é conectado a um grande número de antenas através de um conjunto de deslocadores de fase. Outro fator importante que afeta a qualidade da transmissão é a técnica de modulação usada, que desempenha um papel importante no desempenho do processo de transmissão. O GFDM é um conceito de modulação de portadora múltipla, não ortogonal e flexível, que introduz graus de liberdade adicionais, quando comparado a outras técnicas de portadora múltipla, como o OFDM. Essa flexibilidade faz do GFDM uma solução promissora para as futuras gerações celulares, pois pode atender a diferentes requisitos, como maior eficiência de espectro, melhor controle das emissões fora de banda (OOB), além de atingir baixo rácio de potência média / pico ( PAPR).

Neste trabalho, é assumido uma arquitetura hibrida no transmissor e recetor. Considera-se uma técnica de modulação GFDM a ser implementada na parte digital, enquanto na parte analógica, é proposto um equalizador linear híbrido multiutilizador totalmente conectado, i.e., cada cadeia RF está ligada a todas as antenas, combinado com um pré-codificador híbrido, de baixa complexidade para sistemas MIMO massivo de banda larga. O equalizador híbrido é otimizado, minimizando o erro quadrático médio entre a abordagem híbrida e a contraparte totalmente digital. Os resultados mostram que o desempenho do esquema híbrido proposto está muito próximo do equivalente digital, à medida que o número de cadeias de RF aumenta.

**Keywords** 5G,GFDM, massive MIMO, millimeter-wave communications, hybrid analog-digital architectures,

**Abstract**

Wireless communication using very-large multiple-input multiple-output (MIMO) antennas has been regarded as one of the enabling technologies for the future mobile communication. It refers to the idea of equipping cellular base stations (BSs) with a very large number of antennas giving the possibility to focusing the transmitted signal energy into very short-range areas, which will provide huge improvements in the capacity, in addition to the spectral and energy efficiency. Concurrently, this demand for high data rates and capacity led to the necessity of exploiting the enormous amount of spectrum in the millimeter wave (mmWave) bands. However, the combination of millimeter-wave communications arrays with a massive number of antennas has the potential to dramatically enhance the features of wireless communication. This combination implies high cost and power consumption in the conventional full digital architecture, where each RF chain is dedicated to one antenna. The solution is the use of a hybrid architecture, where a small number of RF chains are connected to a large number of antennas through a network of phase shifters.
On the other hand, another important factor that affect the transmission quality is the modulation technique, which plays an important role in the performance of the transmission process, for instance, GFDM is a flexible non-orthogonal multicarrier modulation concept, that introduces additional degrees of freedom when compared to other multicarrier techniques. This flexibility makes GFDM a promising solution for the future cellular generations, because it can achieve different requirements, such as higher spectrum efficiency, better control of out-of-band (OOB) emissions, as well as achieving low peak to average power ratio (PAPR).

In this work, we present an analog-digital transmitter and receiver structures. Considering a GFDM modulation technique to be implemented in the digital part, while in the analog part, we propose a full connected hybrid multiuser linear equalizer, combined with low complexity hybrid precoder for wideband millimeter-wave massive MIMO systems. The hybrid equalizer is optimized by minimizing the mean square error between the hybrid approach and the full digital counterpart.
The results show that the performance of the proposed hybrid scheme is very close to the full digital counterpart and the gap reduces as the number of RF chains increases.

# Contents

# List of Figures

# List of Tables

# Glossary

| | |
|---|---|
| **GFDM** | Generalized Frequency Division Multiplexing |
| **UFMC** | Universal Filtered Multi Carrier |
| **FBMC** | Filter Bank Multicarrier |
| **IID** | Independent and Identically Distributed |
| **RRC** | Root Raised Cosine |
| **ISI** | Inter-Symbol Interference |
| **ICI** | Inter-Carrier Interference |
| **OFDM** | Orthogonal Frequency Division Multiplexing |
| **WB** | Wideband |
| **1G** | First Generation |
| **2G** | Second Generation |
| **3G** | Third Generation |
| **4G** | Fourth Generation |
| **5G** | Fifth Generation |
| **B5G** | Beyond Fifth Generation |
| **6G** | Sixth Generation |
| **LTE** | Long Term Evolution |
| **AMPS** | Analog Mobile Phone System |
| **OWA** | Open Wireless Architecture |
| **TACS** | Total Access Communication System |
| **OTP** | Open Transport Protocol |
| **LOS** | Line Of Sight |
| **UT** | User Terminal |
| **BS** | Base Station |
| **GSM** | Global System for Mobile Communications |
| **IP** | Internet Protocol |
| **UMTS** | Universal Mobile Telecommunication System |
| **IMT-2000** | International Mobile Telecommunications-2000 |
| **HSDPA** | High Speed Down-link Packet Access |
| **HSUPA** | High speed Up-link Packet Access |
| **EDGE** | Enhanced Data GSM Evolution |
| **WAP** | Wireless Application Protocol |
| **GPRS** | General Packet Radio Services |
| **MQAM** | M-ary Quadrature Amplitude Modulation |
| **DFT** | Discrete Fourier Transform |
| **IDFT** | Inverse Discrete Fourier Transform |
| **MF** | Matched Filter |
| **ZF** | Zero Forcing |
| **MMSE** | Minimum Mean Square Error |
| **AoD** | Angles of Departure |
| **AWGN** | Additive White Gaussian Noise |
| **FFT** | Fast Fourier Transform |
| **IFFT** | Inverse Fast Fourier Transform |
| **MPCs** | Multi Path Components |
| **CP** | Cyclic Prefix |
| **MIMO** | Multiple Input Multiple Output |
| **SISO** | Single Input Single Output |
| **SIMO** | Single Input Multiple Output |
| **MISO** | Multiple Input Single Output |
| **SNR** | Signal to Noise Ratio |
| **CSI** | Channel State Information |
| **mMIMO** | Massive MIMO |
| **PAPR** | Peak-to-Average Power Ratio |
| **OOB** | Out-of-Band Emission |
| **AA** | Antenna Array |
| **2D** | Two-Dimensional |
| **3D** | Three-Dimensional |
| **mmWave** | millimeter Wave |
| **FSL** | Free-Space Loss |
| **RF** | Radio Frequency |
| **DAC** | Digital to Analog Converter |
| **ADC** | Analog to Digital Converter |
| **BER** | Bit Error Rate |
| **ULA** | Uniform Linear Array |
| **QPSK** | Quadrature Phase Shift Keying |
| **IOT** | Internet Of Things |
| **MRC** | Maximal Ratio Combining |

CHAPTER 1

# Introduction

*Wireless Communication has evolved over the past three to four decades, this evolution brought major changes in the type of the used technology, the speed of data transfer, the capacity, and the network coverage. Since the beginning of standardization, each cellular mobile radio generation has been designed to provide specific telecommunications services as an add-ons for the mobile terminal.*
*This chapter provides an overview about the evolution of those generations from the First Generation (1G) to the Fifth Generation (5G). It also describes the motivation, the objectives and the contributions of the proposed work.*

## 1.1 MOBILE TELECOMMUNICATION EVOLUTION

The origins of mobile communications followed quickly behind the invention of radio in the late 1800s. where the radio concept was developed in the first place to be used as communication tools in the navigation domain and safety of ships at sea[1]. Since the early 1970s, the evolution of the mobile wireless industry was initiated, and soon the creation of this technology started to expand. Subsequently in the past few decades, several generations of mobile wireless technologies have been revealed, namely from 1G to 5G .

It all started with 1G mobile system were the cellular concept was firstly introduced and made the large scale mobile wireless communication possible. 1G was used to transmit only the analog signals which made it exclusively suitable for voice service, followed by the 2G mobile technologies replacing the analog technology by digital communications and transmitting digital signals. The Third Generation (3G) technology came after, for the multimedia cell phone or as called typically smart phone, where entertainment services, multimedia, mobile applications and many more features were added. 3G included high data transmission speed compared to Second Generation (2G). Then, followed by the Fourth Generation (4G) which was known as Long Term Evolution (LTE), it basically can do everything 3G can but faster and smoother than ever before. Lastly, 5G mobile technology is

based on Open Wireless Architecture (OWA) and Open Transport Protocol (OTP) and aims to provide high level of services in terms of data rate and capacity.

The following figure illustrates the main difference between mobile generations.

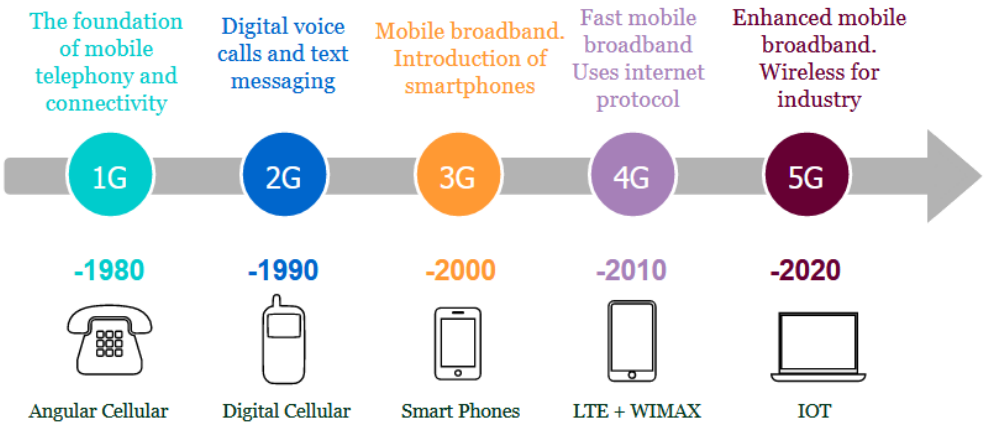


**Figure 1.1:** The evolution of mobile generations

### First Generation 1G

First generation mobile networks were totally reliant upon analog radio systems, based on circuit switched technology. It was designed for voice not for data, which means that users could only make phone calls, they could not send or receive text messages.
The 1G network was first introduced in Japan in 1979 before it was implemented in other countries such as USA in 1980. In USA it was known as Analog Mobile Phone System (AMPS), while in Europe was as typically identified as a variation of Total Access Communication System (TACS),.i.e. different 1G standards were used in various countries.
Voice calls over 1G were modulated at frequencies around 150 MHZ and were transmitted between radio towers. In order to make it work, cell towers were built around the country and the signal coverage could be obtained from greater distances. However, 1G network was unreliable and had some security issues. For instance, cell coverage would often drop, it would experience interference by other radio signals and due to lack of encryption, it could easily be hacked, this means that with a few tools, conversations could be heard and recorded. Comparing to its successors, 1G was only better than the 2G in one point. Namely, due to the analog nature of 1G signals and due to fact that the analog signal are smoother compared to the digital one, a poor quality call made from a 1G handset would gradually worsen, but the same call made from a 2G handset would fail completely [2].

### Second Generation 2G

1G network was not satisfying, the need for better quality, higher capacity, improved coverage, reliability and spectral efficiency paved the way toward second generation cellular systems. 1G was replaced by 2G technology by 1991 when 2G cellular networks were commercially launched on the Global System for Mobile Communications (GSM) standard in Finland and was used by over 2 billion people across more than 212 countries. With this widespread, international roaming between mobile phone operators was affordable, and subscribers became able to use their phones in many parts of the world. As a result, mobile telecommunication industry experienced exponential growth of usage of the both subscribers and valued added services.
This network was planned mainly for voice transmission with digital signal instead of analog, with frequency bandwidth about 20- 200 kHz. It also provided phone conversations encryption, which vastly improved the security and safety. Besides that, it significantly enhanced the spectrum efficiency and introduced data services for mobile, such as message Service where users could send text messages (SMS) and multi-media messages (MMS). Although those services were slow and often without success, but they were digitally encrypted .i.e. the transmitted data could only be reachable and readable by the intentional receiver. Since 2G cellphone units emitted less radio power, they were in general smaller than 1G units. Therefore, another advantage of 2G over 1G was the low consumption of the battery power which made 2G be considered environment friendly, lastly, voice calls over 2G were clearer with less noise and better quality [3][4].

This technology was developed to 2.5G system to achieve higher data rate between 64-115 kbps, based on General Packet Radio Services (GPRS) that was introduced and successfully deployed. Beside Enhanced Data GSM Evolution (EDGE) that is considered a 2.75G and an extended version of GSM, is able to support up to 473.6kbps [5], [1]. 2.5G and 2.75G networks supported services like Wireless Application Protocol (WAP), mobile games and internet communication services such as send/receive emails, web browsing, camera phones [6].

### Third Generation 3G

3G technology was considered as the revolution among radio generations, it combined high speed mobile access with Internet Protocol (IP)-based services, and included features as wireless web base access, multimedia services, email, and video conference.
In comparison to 2G, 3G was much faster, with transmission speed from 144Kbps to 2Mbps, it enabled network operators to transmit greater amounts of data, in order to achieve wide range of services and efficient network capacity. This means that users could video call, share files, surf the internet, watch TV online and play online games on their mobiles for the first

time. Under 3G, cellphones where no longer just about calling and texting, they were the hub of social connectivity with fast data transfer rates as a basic feature. Additionally, it is much flexible, because of its ability to support 5 major radio technologies.
Universal Mobile Telecommunication System (UMTS) was the most important technology proposed by International Mobile Telecommunications-2000 (IMT-2000) as the successor to GSM.

High Speed Down-link Packet Access (HSDPA) is a mobile telephony protocol also called 3.5G. It provided speeds up to 14.4Mbit/s on the down-link and 5.8Mbit/s on the up-link, and improved the performance of the existing UMTS protocols by affording various mobile telephony protocols. High speed Up-link Packet Access (HSUPA) is a complementary of HSDPA, it is advanced person to person data application with higher and symmetric data rate, like email and person to person gaming.
Third generation mobile networks are still in use today, but normally when the superior 4G signal fails. 3G revolutionized mobile connectivity and the capabilities of cellphones[2][3].

**Fourth Generation 4G**

4G refers to the fourth generation of cellular wireless standards. It went one step further than the revolutionary 3G. 4G was planned to fulfil advanced requirements, such as peak data rates up to 1 Gbps at low speeds and up to 100 Mbps at high speeds (five times faster than the 3G network) which means high quality audio/video streaming over end to end IP. Under 4G, users can experience better latency (less buffering), higher voice quality, easy access to instant messaging services and social media, high quality streaming and faster downloads.
Pre-4G technologies such as mobile WiMAX and first-release 3G LTE have been available on the market since 2006 and 2009 respectively. It is basically the extension in the 3G technology with more bandwidth and services offers in the 3G. While first LTE mobile phone appeared in 2010, with many network characteristics such as enabling auto reconfiguration mode. The purpose of 4G systems was not only to support the next generation of mobile service, but also to support the fixed wireless networks [3][7].
To make this system efficient, it is necessary to design new terminals. 4G is considered as a successor standards and the extension of 3G technology with more advanced multimedia services offers and more bandwidth. The development of the standard LTE started in 2004 and became the 4G technology and the first LTE mobile phone appeared in 2010.

**Fifth Generation 5G**

1G, 2G, 3G and 4G were mainly about connecting people, they provided services to allow them connecting each other, or access the internet and use its services. 5G takes the traditional mobile broadband to the extreme in term of data rates, capacity and availability.

With its capabilities of providing very high data rates up to 20 Gbps and higher capacity up to 1000 times, it enables new services such as industrial Internet Of Things (IOT) connectivity and critical communications, which means connecting the applications, appliances, sensors, objects, and devices with the internet and this requires transmitting, collecting, analyzing and processing data in an efficient network. Moreover, health care can be included in the features of 5G in terms of the use of a smart medical devices able to make remote surgery. 5G aims to present major steps in mobile network capacity and performance due to its flexible platforms for device connectivity, ultra-low latency and high reliability with much less limitations and obstacles among the previous generations. It is expected that 5G can essentially affect all sections of society by improving efficiency, productivity and safety, aiming to spread the concept of the cloud in wireless networks, and rapidly increase the use of artificial intelligent and machine learning. 5G design and deployment need to be different from the earlier mobile network generations because of the new requirements. Therefore, a number of new technologies are needed to fulfil those targets like the use of Massive MIMO (mMIMO) beamforming and millimeter Wave (mmWave) bands to exploit the frequency spectrum, in order to achieve high data rates and capacity.
Figure 1.2 summarizes the use of 5G and its features, they can further be summarized as: providing high security and reliability with low latency in the order of milliseconds to achieve ultra-fast mobile Internet, besides achieving a high broadcasting data (in Gbps) in terms of supporting almost 65000 connections.

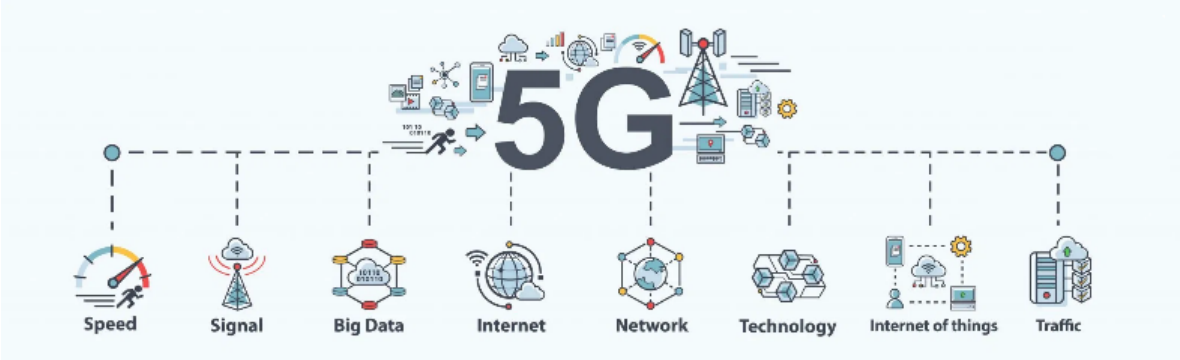


**Figure 1.2:** 5G main features

Researches are still expanding at the meantime aiming to reach the best technologies toward the next generations of wireless communications beyond 5G or Sixth Generation (6G), mainly achieving higher data rates and frequency capacity. Their aspiration is to overcome and solve the problems that were facing the previous generations especially in the areas that 5G is not able to achieve [8].

## 1.2 MOTIVATION AND OBJECTIVES

Orthogonal Frequency Division Multiplexing (OFDM) has been also considered for 5G systems, due to its advantage over single carrier schemes, namely ability to cope with severe

channel conditions. However, because of OFDM imperfections such as the need for precise synchronization and the large Peak-to-Average Power Ratio (PAPR), in addition to the limitation in its spectrum efficiency caused by the requirement for Cyclic Prefix (CP) in every OFDM symbol, it became unsuitable for future requirements. Consequently, new multi carrier transmission schemes were revealed to address these problems. Filter Bank Multicarrier (FBMC), Universal Filtered Multi Carrier (UFMC), and Generalized Frequency Division Multiplexing (GFDM) are new promising techniques for Beyond Fifth Generation (B5G) and 6G applications.

GFDM is the most flexible non-orthogonal multi carrier transmission scheme compared to the other multi carrier modulations techniques, it is the generalization of OFDM. GFDM is based on traditional filter bank multi-branch multi carrier concepts which are now implemented digitally. It has several added advantages including lower PAPR, ultra-low Out-of-Band Emission (OOB) radiation due adjustable Tx-filtering and last but not least a block-based cyclic prefix insertion to allow for low complex equalization at the receiver side. GFDM enables frequency and time domain multi-user scheduling comparable to OFDM and provides an efficient alternative for white space aggregation even in heavily fragmented spectrum regions. On the other hand, GFDM and its flexible characteristics fulfils the requirements to be combined with Massive Multiple Input Multiple Output (MIMO) technology, which in turn regarded as a key promising technology for 5G wireless networks, where it enables packing massive number of antennas and focus energy to brings drastic improvements in throughput and efficiency.

Another important required aspect is the mmWave frequencies. The small wavelength allows the use of mMIMO technique where it is allowed compacting more antennas in the same space compared to current microwave communication systems [9]. Therefore, the combination of mMIMO with mmWave is highly attractive because it offers potentials to significantly raise user throughput, enhance spectral and energy efficiencies and increase the capacity of mobile networks. This combination uses the joint capabilities of the huge available bandwidth in the mmWave frequency bands and high multiplexing gains achievable with massive antenna arrays over the current 4G cellular networks at current cell densities [10], it also overcompensate the propagation difficulties of mmWave communications [11]. Along with the increased number of antennas, both the network and mobile devices implement more complex designs and hardware limitations to coordinate mMIMO operations. Therefore, the idea of implementing hybrid architectures is widely proposed recently, where part of signal processing is done at the analog domain and a reduced complexity processing is left to the digital domain [12][13]. Which in turn put challenges to develop new algorithms in order to adapt with the demands of these high complex composite technologies.

The main objective of this work is designing an efficient hybrid equalizer combined with low complexity hybrid precoder for Wideband (WB) mmWave mMIMO system. For the analog part, we propose an algorithm designed for fully connected architecture, where each Radio Frequency (RF) chain is connected to all antennas. While in the digital part, GFDM modulation is performed, and the signal is transmitted over WB mmWave channel.

The performance of this proposal is tested over many scenarios according to the number of antennas and the number of RF chains and compared with the full digital counterpart of every case. The results show that the performance of the proposed hybrid scheme is very close to the full digital counterpart and the gap reduces as the number of RF chains increases.

## 1.3 CONTRIBUTIONS

The main contributions of the research performed in this dissertation include novel efficient full-connected hybrid analog-digital transmit and receive schemes for mmWave mMIMO systems in a combination with GFDM modulation technique, that has originated the following publications:

**Journal Paper**

J. Kassam, M. Miri, R. M. Magueta, D. Castanheira, A. Silva, A. Gameiro, "Two-Step Multiuser Equalization for Hybrid mmWave Massive MIMO GFDM Systems", Electronics, July, 2020.

**Conference Paper**

J. Kassam, M. Miri, R. M. Magueta, D. Castanheira, A. Silva, A. Gameiro, "Hybrid Multiuser Equalizer for mmWave Massive MIMO GFDM Systems", in proceeding of 12th IEEE/IET International Symposium on Communication Systems, Networks and Digital Signal Processing-CSNDSP, Porto, Portugal, July, 2020.

## 1.4 STRUCTURE OF THE DISSERTATION

This document is organized into five chapters, as described below:

**Chapter 2** starts by presenting an overview about the radio propagation basic concepts including propagation mechanisms and impairments. Then it describes channel models characteristics and fading concept, in addition to fading types and specifications and its affects on the signal propagation. Then a survey about OFDM and GFDM modulation schemes are described in details.

**Chapter 3** starts by an overview about the diversity concept and leads to introduce the MIMO systems and the extending to massive MIMO. After that a brief review about a future wireless systems concept is provided, namely mmWave and the combination with the mMIMO. Then, a description about clustered WB channel model for mmWave mMIMO is presented. Lastly, the hybrid architectures properties and specifications are presented.

**Chapter 4** presents the description of the implemented GFDM based hybrid equalizer combined with the low complexity hybrid precoder for WB mmWave mMIMO systems. Starting with the system characterization, the transmitted and receiver model and lastly the

equalization scheme. Later, the proposed solution is evaluated under a realistic mmWave channel model.

**Chapter 5** summarizes the main conclusions and possible future work .

CHAPTER 2

# Background and Basics

*This chapter covers some of the most basic concepts related to the wireless system in terms of the propagation techniques and the constraints that face the signal propagation, beside explaining some wireless channel models specifications. It also introduces the modulation schemes that are needed to understand the work developed in this dissertation.*

## 2.1 PROPAGATION BASIC CONCEPTS

The electromagnetic wave propagation is the main definition of the "wireless" communications. These sinusoidal waves are formed of both a time varying electric and magnetic field. The number of times that the radio wave oscillates per second refers to the frequency which is one of the main characteristics of the wave. Radio waves are type of waves in the electromagnetic spectrum, the waves with the lowest frequencies, they are used in wireless communication to carry the signals. They radiate from an antenna and propagate through a channel between a transmitter and a receiver.

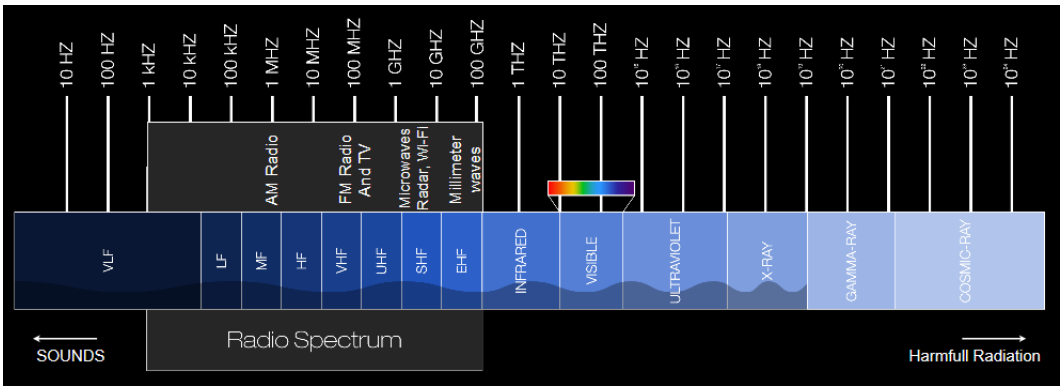


**Figure 2.1:** Electromagnetic spectrum

### 2.1.1 Radio Waves Propagation Mechanism

The signal can be transferred from the transmitter to the receiver via several different propagation paths, sometimes there is a Line Of Sight (LOS) between them but in the typical mobile environment LOS is missing, and in this case the signal is transmitted by means of being reflected at or diffracted by different objects in the environment: houses, mountains (in some hilly areas), windows, walls and so on, as shown in figure 2.2. [6]. Mainly the propagation mechanism can be described as [14]:

**Scattering** occurs when a radio wave hits an irregular shape item smaller than the wavelength of the signal such as street signs and lamp posts and foliage. The radio wave in this case reflects in multiple directions and loses energy, but it reaches the receiver from approximately the same direction with slight differences in delay.

**Reflection results** when a radio wave impinges on an object that is larger than the wavelength of the radio signal like a wall. Thus, the radio wave bounces off the surface. An example would be radio waves bouncing off walls.

**Refraction** occurs when a radio wave meets an object with a density different to the one of its medium. This causes a propagation of the radio wave at a different angle. The propagation of the radio waves through clouds is an example of the refraction.

**Diffraction** arises when an object with sharp irregular edges, like a building, blocks the radio wave, thus the radio wave splits and creates diffracted signals from the original one, so they bend around the corners of the object. It is this property that allows radio waves to operate without a direct line of sight.

**Absorption** results when a radio wave passes through an object causing and absorption of a part of its strength, it comes from the other side weaker. An example is a radio waves going through trees.

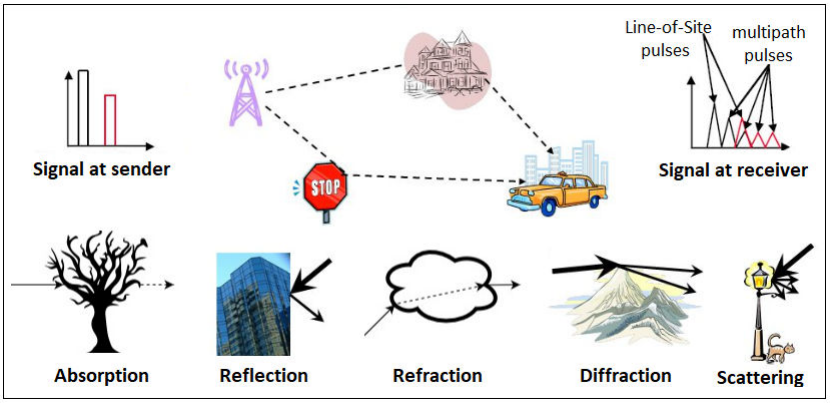


**Figure 2.2:** Radio wave propagation mechanisms

### 2.1.2 Radio Waves Propagation impairments

Many problems may occur during the transmission of a radio signal. Some of the most common problems are described below [1].

**Path loss:** is caused by dissipation of the power radiated by the transmitter as well as effects of the propagation channel; it occurs when the received signal becomes weaker and weaker due to the increasing distance between the transmitter and the receiver, even if there are no obstacles between them.

**Shadowing:** Occurs when a shadowing effect is created by a physical obstacle like a hill or a building between the transmitter and the receiver. Which can attenuate the received signal power.

**Multi path fading:** It happens because there is more than one propagation route to the receiver, therefore more than one signal arrives at the receiver. This may be due to buildings or mountains, either close to or far from the receiving device.

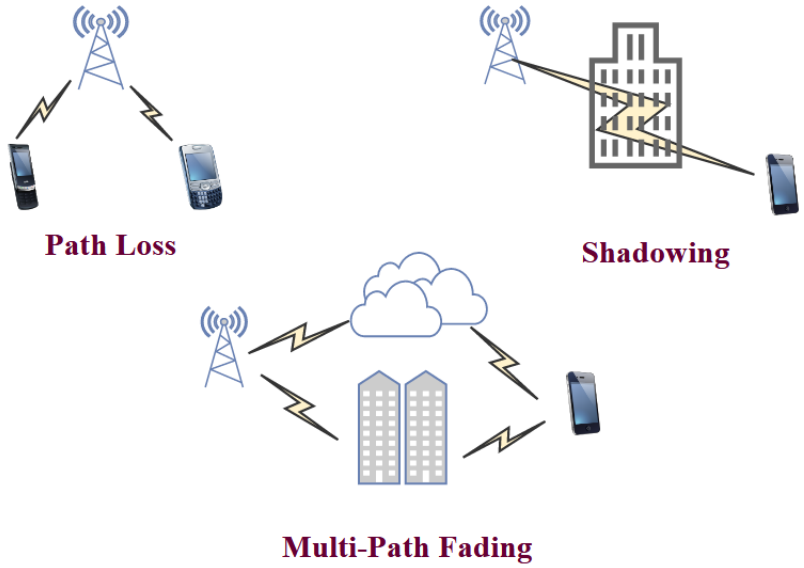


**Figure 2.3:** Radio waves propagation impairments

In wireless communication environment, many copies of the transmitted signal reach the receiver side, some of them constructively combines and some of them destructively combines. Therefore, the final version of the received signal becomes drastically different from the original transmitted one and usually poorer. This type of signal deterioration is called 'Fading'. The combination between the propagation factors generates different fading effects. For instance, figure 2.4 illustrates real observed fading as a result of 3 major components: path-loss, shadowing and multi-path[15].

On the left side, the first plot shows the path-loss which decreases gradually but not

obviously fluctuates. In the second plot, the fluctuation of the signal is more apparent but not very strong. While in the third plot, it is the strongest among the others. Hence, the right side presents the real received signal as a result of the effect of those three components.

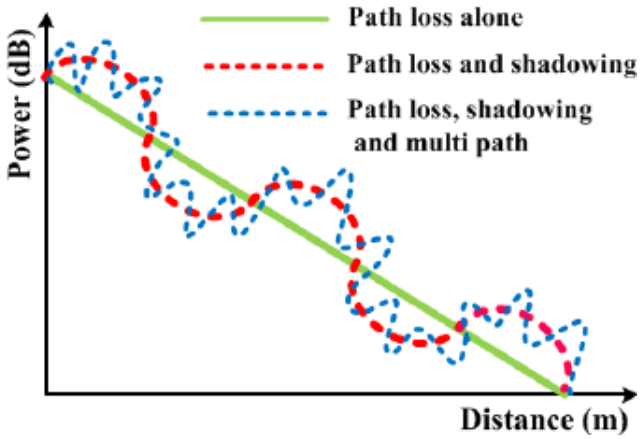


**Figure 2.4:** Fading components [16]

### 2.1.3 Fading Types

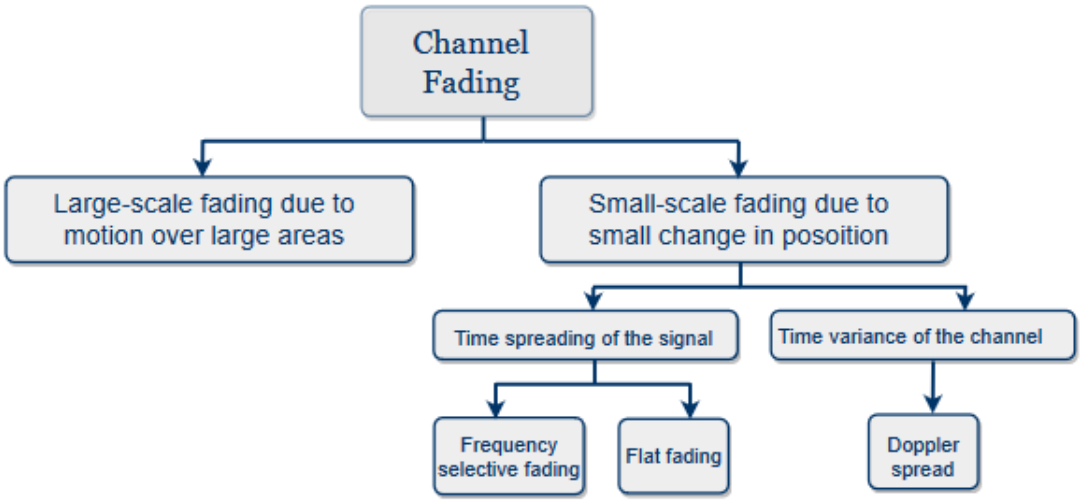


**Figure 2.5:** Channel fading types

The fading phenomena is categorized into two main groups known as large scale fading and small scale fading. The large scale fading is used to describe the signal level at the receiver after traveling across a large area (hundreds of wavelengths) and can be characterized by the distance between transmitter and receiver. Small scale fading describes the signal level at the receiver after encountering obstacles near (several wavelengths to fractions of wavelengths) the receiver, it basically implies to the short-term, rapid amplitude fluctuations

of the received signal during a short period of time due to small changes in position (as small as half wavelength) or to changes in the environment [17][18].

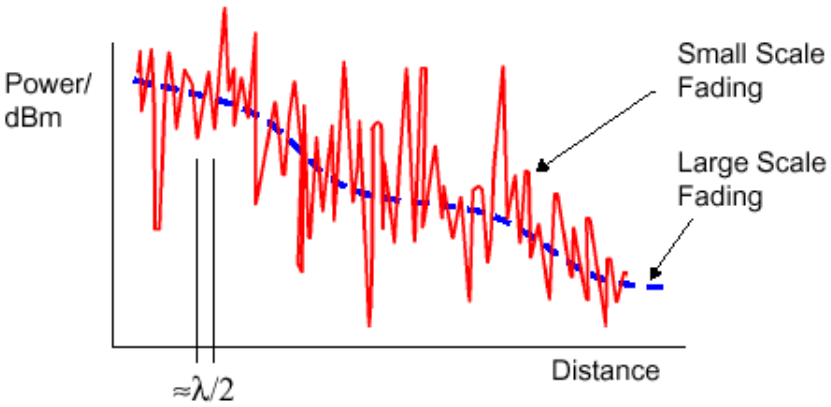


**Figure 2.6:** Small scale fading and large scale fading [19]

**Small Scale Propagation Models:**
Many small-scale fading types can be caused by different channel conditions and behaviors. Two main factors can influence it:

- Time Delay Spreading of the Signal: This factor can be classified as either flat fading or frequency selective spreading; where the small delay spread gives rise to flat fading and the large delay spread brings about frequency selective fading [14].

  **Flat fading**
  Small-scale fading is defined as being flat or non-selective if the coherent bandwidth is greater than the bandwidth of the transmitted signal, in other words the received multi path components of a symbol do not extend beyond the symbol's time duration. Hence, channel Inter-Symbol Interference (ISI) is absent.
  Flat-fading channels are also known as amplitude varying channels, and they are sometimes referred to as narrow band channels, since we are applying a narrow signal bandwidth compared to the channel bandwidth. If we are transmitting a signal with a bandwidth $B$ across a channel and assuming $B_c$ is the coherence bandwidth of the channel, we can describe the main characteristic of flat fading as $B \ll B_c$. And fading is roughly correlated across the entire signal bandwidth.

  **Frequency-Selective Fading**
  In contrast to flat fading, when the coherence bandwidth of the channel $B_c$ is smaller than the bandwidth of the transmitted signal $B$: $B \gg B_c$ we experience frequency selective fading on the received signal. When this occurs, the received signal includes multiple versions of attenuation and delay on the same symbol. Accordingly, the channel experiences ISI. In the frequency domain, this means that certain frequency components in the received signal spectrum have larger gains than others [20].

The following figure illustrates the difference between the discussed cases, it shows two superimposed signals, flat-fading and frequency selective fading.

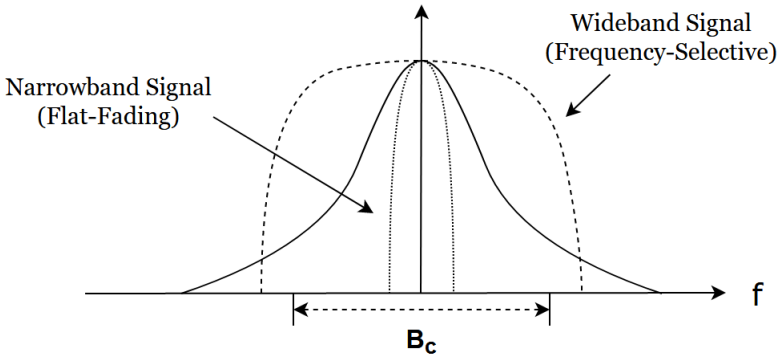


**Figure 2.7:** Wide band and narrow band with coherence bandwidth $B_c$

- Time-Variant Behavior of the Channel: The mobility of a transmitter or a receiver leads to time variant of the channel which in turn causes Doppler shift[20]. Doppler shifts phenomena in communication transmission can be expressed as Doppler spread. The Doppler spread defines the signal fading and variation behavior. which is related to the wavelength of the transmitted signal, and the UT movement. It can be calculated based on the speed of the mobile, the direction of motion and the angle of arrival of the signal. Consequently, using the Doppler information can improve the performance and reduce the complexity at the receiver side [21].

It is important not to confuse the terms with the terms large-scale and small-scale fading fast- and slow-fading. We must emphasize that fast- and slow-fading deal with the relationship between the time rate of change in the channel and transmitted signal, and not with the propagation path-loss models. Particularly, Fast Fading describes a condition where the time duration in which the channel behaves in a correlated manner is short compared to the time duration of a symbol. While in slow fading, the time duration that the channel behaves in a correlated manner is long compared to the time duration of a transmission symbol [22].

## 2.2 FADING DISTRIBUTIONS

Each multipath propagation channel has its has own characteristics. Small fluctuations of the signal in a time-varying linear channel can be described as a Rayleigh fading. In case of a large number of paths, the envelope of the received signal may be statistically described by Rayleigh distribution or Rician distribution for the cases with no LOS and LOS components, respectively [14] [23].

- **Rayleigh Channel Model**
  Fading can be modeled as Rayleigh if the number of multiple reflective paths is large and

there is no main LOS path between the transmitter and the receiver. It has coefficients Independent and Identically Distributed (IID) and it is usually expressed as a zero mean complex Gaussian variable with unit variance. The Rayleigh distribution has a probability density function given by:

$$f(r) = \frac{r}{\sigma^2} e^{-\frac{r^2}{2\sigma^2}}, \tag{2.1}$$

where $\sigma^2$ is the variance of the received signal $r$. Another mode to view the Rayleigh distribution is as the probability density function of the received signal amplitude to the noise ratio, which is proportional to the square of the signal envelope. Let $A$ be the receiver signal-to-noise ratio; the probability density function of $A$ is exponential [24] and can be written as:

$$p_A(a) = \frac{1}{\rho} e^{\left(\frac{a}{\rho}\right)} \qquad a \geqslant 0 \tag{2.2}$$

where $\rho = E[A]$.

- **Rician Channel Model**
  The small-scale fading when a LOS propagation path does exist is described by the Rician distribution. In this case, the signal appears as a continuous component added with a random multi-path component.
  Rician distribution is given by

$$p(r) = \frac{r}{\sigma^2} e^{-\frac{r^2+\upsilon^2}{2\sigma^2}} I_0\left(\frac{r\upsilon}{\sigma^2}\right), \tag{2.3}$$

  where $\upsilon$ denotes the peak amplitude of the dominant signal and $I_0$ is the modified Bessel function of the first kind and zero order. The Rician distribution is often described in terms of a parameter $K$, which is the ratio between the deterministic signal power and the variance of the multi-path component:

$$K = \frac{\upsilon^2}{2\sigma^2} \tag{2.4}$$

  The parameter $K$ completely specifies the Rician distribution. For $K = 0$, the Rician distribution reduces to a Rayleigh distribution. As shown in the following figure:

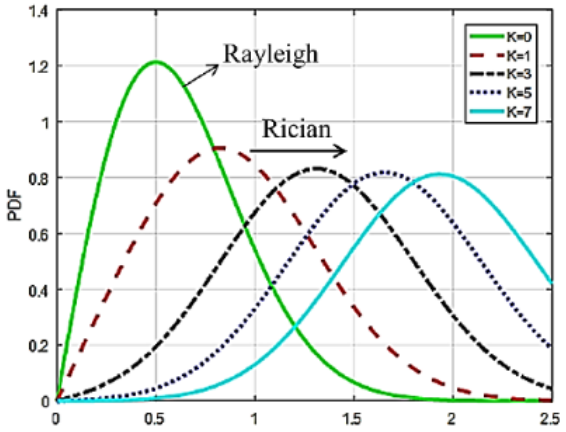


**Figure 2.8:** Rayleigh and Rician power distribution [25]

## 2.3 MODULATION SCHEMES

In this Section we start by presenting the OFDM modulation, which is a very popular multicarrier technique that has been used within current wireless technologies, and was considered in 5G technology. After that, we address the GFDM, which is a filtered multi-carrier approach, considered as the generalization of OFDM, and has many advantages over OFDM, since it allows controlling the OOB emissions and the PAPR.

### 2.3.1 Orthogonal Frequency Division Multiplexing (OFDM)

A multi carrier system approach basically relies on dividing the data signal into different sub-streams and sending each of them by a different sub carrier, each one of these sub carriers is made orthogonal to one another. Thus, each of these sub streams occupies a lower bandwidth as well as needs lower data rate, the respective sub-channel can be considered flat. As we can see in figure 2.9

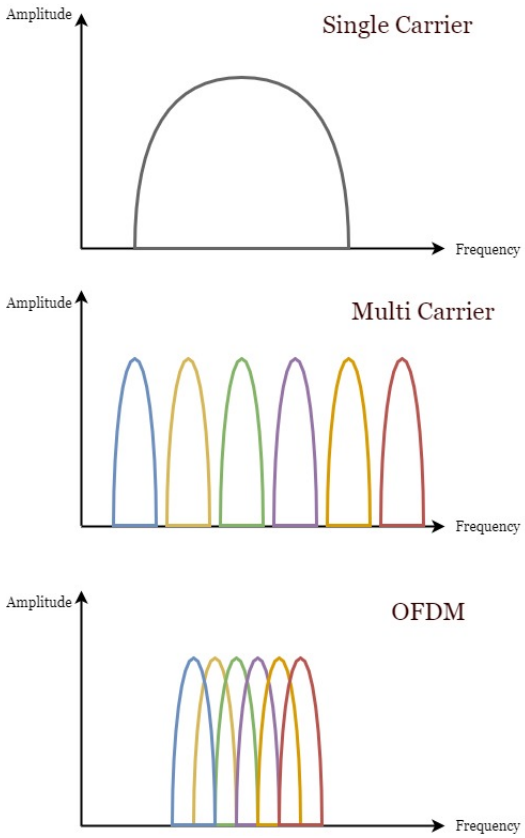


**Figure 2.9:** Spectrum comparison between single and multi carrier systems

OFDM is a special case of multi carrier transmission where a single data stream is transmitted over a number of lower-rate sub carriers, it has many advantages over single carrier systems, mainly the good performance in critical channel conditions, such as narrow band interference and frequency-selective fading due to multi path, without a complex equalizer. The most essential characteristic is the orthogonality between the carriers, it is the main goal behind applying OFDM because this helps in increasing the overall spectral efficiency of the system where there is no Inter-Carrier Interference (ICI) between closely spaced carriers. Since the data will be transmitted over independent carriers with different phase and amplitude requirements for each, it is necessary to choose the required spectrum that depends on the input bits data and the type of digital modulation.
Thus, to ensure the orthogonality between the chosen carrier frequencies, the Inverse Fast Fourier Transform (IFFT) and Fast Fourier Transform (FFT) operations are considered the key to achieving that [14][26][27].

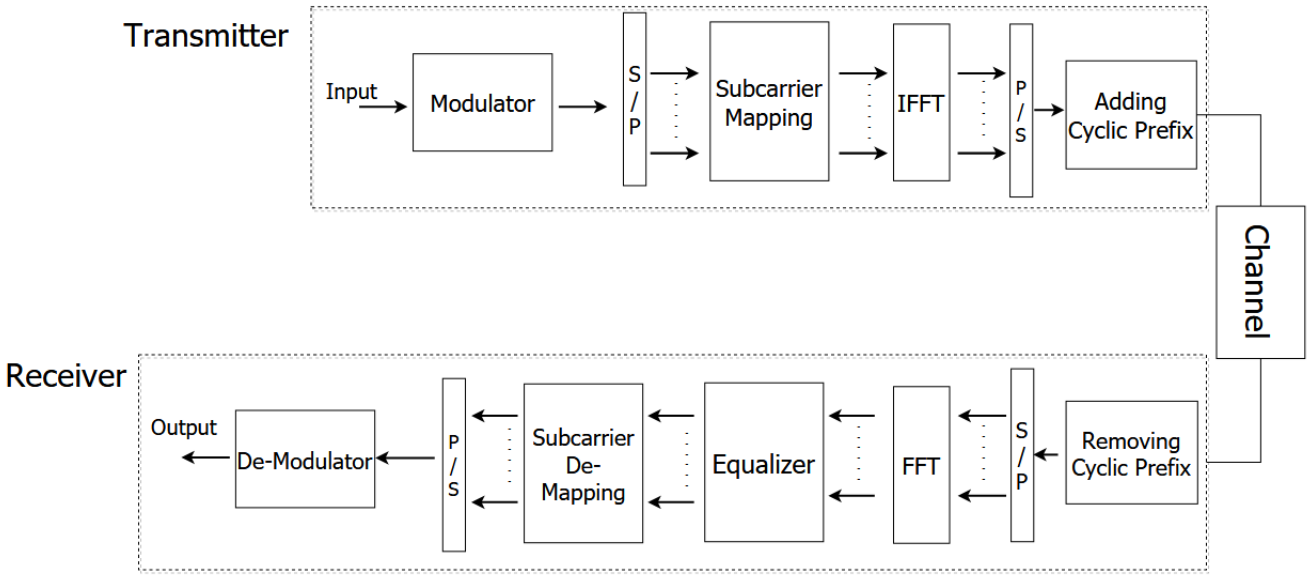


**Figure 2.10:** OFDM transmitter/receiver block diagram

The block diagram of OFDM is presented in figure 2.10 At the transmitter, the input bit stream is modulated into data symbols, and converted to parallel bits by serial-to-parallel conversion block. Then, these bits are mapped into the OFDM frame before a Nc-point IFFT is applied. Lastly, CP is added to eliminate the ISI and ICI at the receiver caused by the multi path delay spread in the channel.

At the receiver, the CP which was inserted between each of the symbols is removed at the first place, then a serial to parallel conversion is performed to divide the series of symbols into several parallel ones and a Nc-point FFT is applied. After that, the equalizer is applied in the infrequency domain to remove the effects of channel, followed by performing the de-mapping operation and data demodulation.

Starting by the data modulation process by $N_c$ sub carriers $f_0, .., f_k, .., f_{N_c-1}$, the spacing between sub carriers is $\Delta f = \frac{B}{N_c}$, where $B$ is the bandwidth. OFDM symbol duration in a sub carrier is given by

$$T_{OFDM} = \frac{1}{\Delta f} = \frac{N_c}{B}. \tag{2.5}$$

we can observe from (2.5), that the symbol duration is bigger than the delay spread , which means that the channel is less sensitive to fading, channel distortion and ISI. The orthogonality between sub carriers requires to fulfil a typical case, that $\Delta f T_{OFDM}^{-1}$ should be equal to one, as showed in (2.5). This condition arises because the OFDM symbol pulse is shaped by a square wave in the time domain, which is a sinc wave in the frequency domain [28].

Therefore, as seen in figure 2.11, when we choose a multiple of the nulls in the spectrum of one sub carrier line up with the peaks of the adjacent sub carriers [29]. In this way, we have a good spectral efficiency and no interference, allowing to recover the original signal.

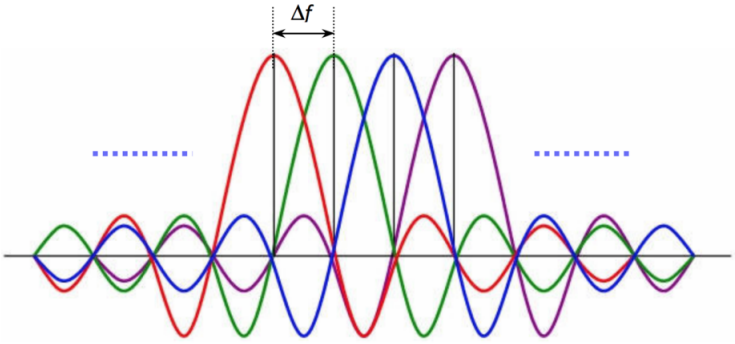


**Figure 2.11:** Orthogonality of OFDM signal subcarriers [30]

The received signal is

$$r(t) = \mathrm{Re}\left[\sum_{k=0}^{N_c-1} s_k \mathrm{rect}(t/T_{OFDM}) e^{j2\pi kt/T_{OFDM}} e^{j2\pi f_c t}\right], \tag{2.6}$$

where $s_k \in \mathbb{C}$ is a data symbol from a given constellation, and $f_c$ is the RF carrier. The function rect(.) is the rectangular pulse shaping function. Removing the RF carrier, we obtain the base band signal, given by

$$c(t) = r(t)e^{j2\pi f_c t} = \sum_{k=0}^{N_c-1} s_k e^{j2\pi kt/T_{OFDM}}. \tag{2.7}$$

Finally, if we sample the signal $c(t)$ at a rate $N_c/T_{OFDM}$ , we obtain

$$c_n = c(nT_{OFDM}/N_c) = \frac{1}{\sqrt{N_c}} \sum_{k=0}^{N_c-1} s_k e^{j\left(2\pi \frac{f_k}{B}\right)n}, \tag{2.8}$$

where$f_k = k\Delta f$, $n = 0, ...., N_c-1$, which coincides with the Inverse Discrete Fourier Transform (IDFT), i.e., Therefore, to demodulate the data at receiver side, it is only needed to apply the Discrete Fourier Transform (DFT), which may be efficiently calculated using the fast Fourier transform FFT algorithm. As mentioned above, a CP is added to the transmitted signal. The CP is a copy of the last part of the OFDM symbol, which is attached in the beginning of symbol, and it makes the channel circular. The CP is used because in a time-disperse channel, the OFDM symbol can lose their orthogonality which causes ISI [31]. The length of CP should be greater than the maximum delay spread of the channel where in this case the length of symbols will be extended, otherwise we will have ISI, [32]. As we can see in figure 2.12,(b) illustrates how the efficient length of the CP can prevent the occurrence of ISI, which is obvious in (a) where the length of CP is less than the length of the delay spread.

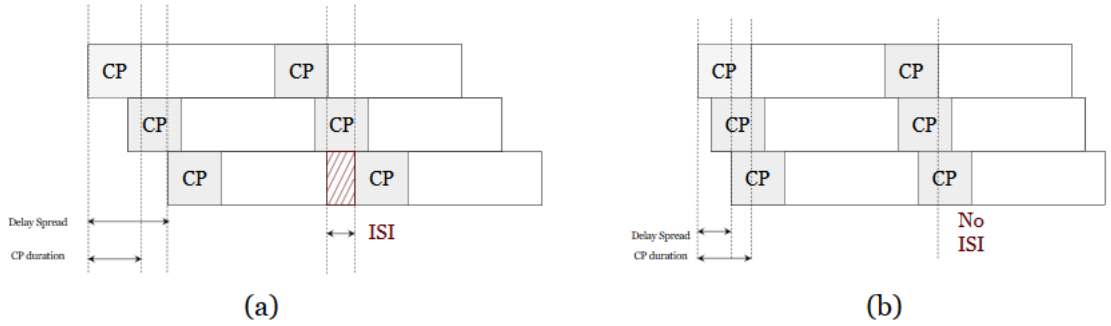


**Figure 2.12:** CP length effect on OFDM symbols

Additionally, the OFDM symbol duration increases when the CP duration also increases, then we cannot increase the CP duration as much as we want or then the transmission rate is reduced. Finally, to avoid the ICI, we need the spacing between sub carriers, to be much higher than the maximum Doppler shift [33].
The main problem of OFDM is the large PAPR, which requires the use of power amplifiers with a very high linear range to avoid signal distortions, which make the system performance lower[27].

### 2.3.2 Generalized Frequency Division Multiplexing (GFDM)

GFDM is also one of the waveform candidates for beyond 5G cellular networks. It is a generalized form of OFDM but here the carriers are not orthogonal to each other, and thus it is considered as the most flexible digital multi carrier scheme.
The main principle of GFDM is dividing the input bits stream into several sub carriers and several sub symbols. For each sub carrier, the impulse response of the pulse shaping filter will apply circularly. Therefore, the sub carrier filtering reduces the OOB emissions and the PAPR, but the ICI will increase and cause a degradation in the performance of the GFDM system [32][34][35]. In this system, the input bit streams is divided into sequence of complex valued data symbols, each sequence (as a vector) is spread on sub carriers and time slots. Therefore, each GFDM frame is indexed by sub carriers and data symbols [35] as

$$\mathbf{D} = \begin{pmatrix} d_0 \\ d_1 \\ \vdots \\ d_{K-1} \end{pmatrix} = \begin{pmatrix} d_0[0] & \cdots & d_0[M-1] \\ \vdots & & \vdots \\ d_{K-1}[0] & \cdots & d_{K-1}[M-1] \end{pmatrix}, \tag{2.9}$$

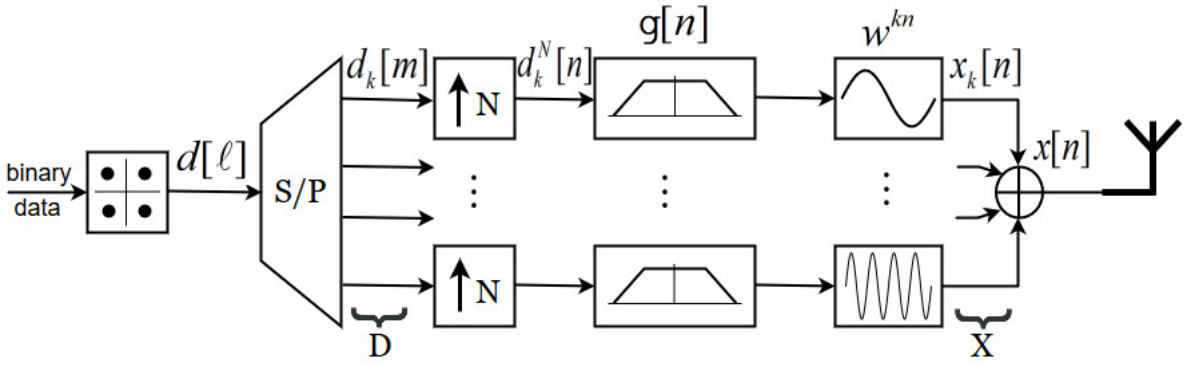


**Figure 2.13:** GFDM Transmitter System Model [35]

**In the transmitter model**, see figure 2.13, we present the process, starting by up-sampling the complex-valued data symbols by zero-padding zeros

$$d_k^N[n] = \sum_{m=0}^{M-1} d_k[m]\delta[n - mN], \tag{2.10}$$

where $\delta(.)$ is the Dirac function and $N$ is the number of samples (up-sampling factor). Then by using a circular convolution $\circledast$ , a pulse shaping filter $g[n]$ with the length of filter $L \leqslant M$ is applied on the transmitted samples $d_k^N[n]$ , where $n = 0, ..., MN - 1$ is the sample index and $N \geqslant K$ to avoid the aliasing, which means that in case of increasing the length of $g[n]$ this will allow the sampling rate to be increased [36]. Thus, the resulting signal is shifted by a sub ccarrier center frequency $w^{kn} = e^{j\frac{2\pi}{N}kn}$ where $\frac{1}{N}$ is the sub carrier spacing. The resulting sub carrier transmit signal $x_k[n]$ can be formulated [35] as

$$x_k[n] = (d_k^N \circledast g)[n].w^{kn}, \tag{2.11}$$

and expressed in a block structure as

$$\mathbf{X} = \begin{pmatrix} \mathrm{x}_0 \\ \mathrm{x}_1 \\ \vdots \\ \mathrm{x}_{K-1} \end{pmatrix} = \begin{pmatrix} x_0[0] & \cdots & x_0[M-1] \\ \vdots & & \vdots \\ x_{K-1}[0] & \cdots & x_{K-1}[M-1] \end{pmatrix}. \tag{2.12}$$

In the result, the transmitted signal $x[n]$ of GFDM is obtained by summing up all sub-carrier signals as given

$$x[n] = \sum_{k=0}^{K-1} x_k[n]. \tag{2.13}$$

Initially, the transmitter and the receiver will be operated in ideal concurrency, which means without regard to any channel and noise. Consequently, the received signal is equal to the transmitted signal $y[n] = x[n]$.

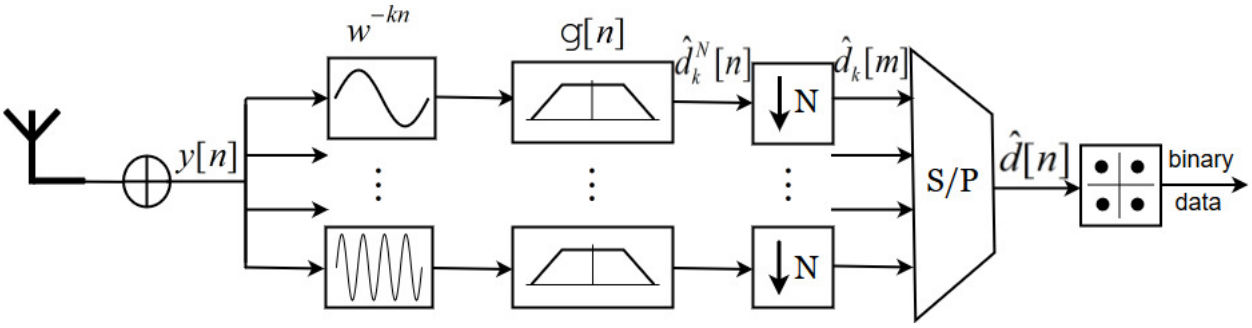


**Figure 2.14:** GFDM Receiver System Model [35]

**In the receiver model**, the received data symbols $\hat{d}_k[m]$ of Matched Filter approach for GFDM system [35] is obtained first by applying a digital down conversion $w^{-kn} = e^{-j\frac{2\pi}{N}kn}$ on the received signal $y[n]$ as

$$\hat{y}_k[n] = y[n].w^{-kn}. \tag{2.14}$$

Then, using the circular convolution operator $\circledast$ to convolve the signal with the receiver filter

$$\hat{d}_k^N[n] = (\hat{y}_k \circledast g)[n]. \tag{2.15}$$

After that, the down sampling technique is performed according to

$$\hat{d}_k[m] = \hat{d}_k^N[n = mN]. \tag{2.16}$$

Finally, the received symbols $\hat{d}_k[m]$ are de-mapped to produce a sequence of bits $\hat{d}[n]$. GFDM loses the orthogonality between the sub carriers and thus it is needed to employ complex equalizers to remove the interference. In the case of using Root Raised Cosine (RRC) filters in the transmitter and the receiver sides, only the adjacent sub carriers interfere causing ICI [35] as shown in figure 2.15,

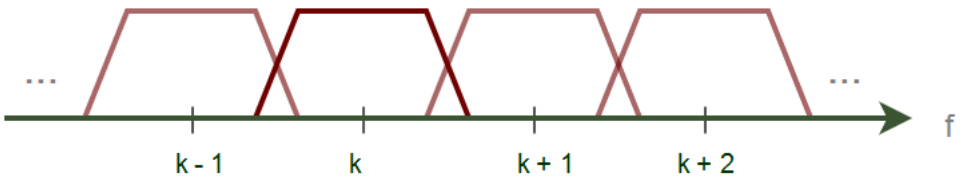


**Figure 2.15:** The self-interference in the $k$th sub carrier from adjacent sub carriers

This figure 2.15 shows the interference of data between the adjacent sub carriers in the frequency domain and more detail will be given in 4. In this work, we are using GFDM as the used modulation scheme due to its benefits regarding reducing PAPR and the OOB emissions.

CHAPTER 3

# Multiple Antennas Systems

*The expansion of the capacity and reliability of wireless communication systems using multiple antennas has been an attractive field of research for more than 20 years. Typical MIMO installations use access points or BSs with relatively few (i.e., less than 10) antennas, and the corresponding improvement in spectral efficiency has been relatively modest. To achieve more dramatic gains, a grander view of the MIMO concept envisions the use of orders of more antennas (e.g., 100 or more) at each BS, a concept often referred to as massive MIMO.*

## 3.1 DIVERSITY IN WIRELESS COMMUNICATION

One of the biggest challenges we have in wireless communications is the channel fading, due to random signal attenuation and phase distortions from Multi Path Components (MPCs) [37]. In order to protect the signal from any kind of fading and enhance the reliability of the signals, some diversity techniques are used. We mainly describe diversity by transmitting and receiving many versions of the message signal through different independent paths [38]. The statistic independence between the transmitted signals reduce the probability of receiving several replicas of the same message signal. However, this technique can be efficient even with the exist of some correlation among the received signals of the same message signal [14].

### 3.1.1 Diversity techniques

Diversity techniques have significant impact over signal fading beside many other effects [14]:

1. Increasing the message reliability at relatively low cost.
2. Reducing the transmit power on the reverse link, which is important to protect the link during the short intervals of deep fading.
3. Improving voice quality and hand-off performance due to the low-signal outage.
4. Improving the frequency-reuse factor and system capacity by decreasing the variability of carrier-to-interference ratio.

5. Antenna diversity increases the received signal strength by taking advantage of the natural properties of radio waves [1].

There are various techniques to achieve diversity, such as time diversity, space diversity, site diversity, frequency diversity, polarization diversity, angle diversity, and path diversity. The combination of the different diversity techniques and how signals are combined define the performance of diversity [14].

**Space diversity:** This type is widely used in mobile radio base stations, because of its simple implementation. It benefits from the random nature of propagation in different directions, like propagation environment characteristics by employing multiple antennas at the transmitter and/or receiver to create spatial channels. For instance, we can increase the strength of the received signal at the Base Station (BS) by mounting two receiver antennas instead of one. If the two Rx antennae are physically separated, it is improbable that all the channels will fade simultaneously. By selecting the best of each signal, the impact of fading can be reduced [14].

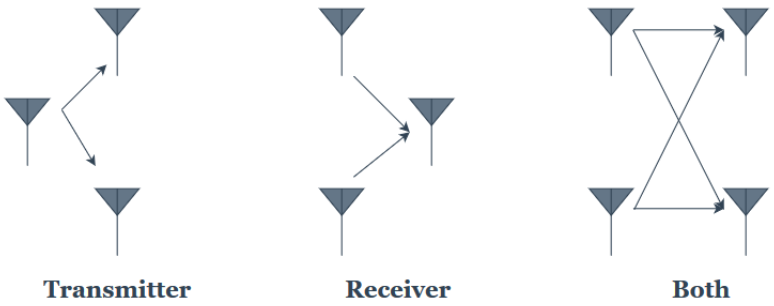


**Figure 3.1:** Space Diversity

**Time Diversity:** Time diversity means transmitting the signal many times in different time periods, using time intervals longer than the fade duration to separate the transmitted signals. Therefore, the copies of the message signal experience independent fading. Time diversity is more functional when the coherence time of the channel is less than time separation between transmissions. However, when neither the transmit end nor the receive end is on the move, time diversity is not very effective, as the coherence can be quite long. This makes it not suitable for delay sensitive applications, like voice communications. It requires storage and additional processing such as interleaving, and it occupies larger bandwidth because of sending the signal many times which lead to a decrease in the data rate [14].

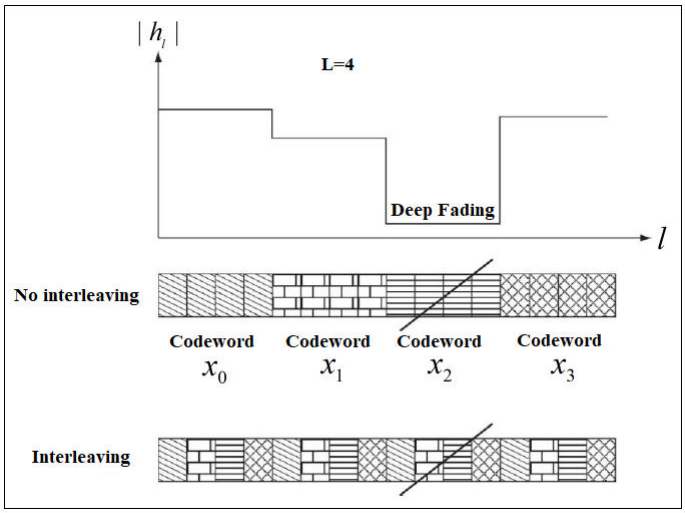


**Figure 3.2:** Time Diversity [39]

**Frequency Diversity:** Frequency diversity is more complex and more costly than space diversity, it requires two transmitters at the near end of the link. The transmitters are modulated simultaneously by the same signal but transmit on different frequencies. Hence, if one signal experienced fading, the fading probably will not occur to the other one. The carriers are separated by the coherence bandwidth of the channel, i.e. the carrier frequencies should have greater separation than the coherence bandwidth of the radio channel. The more one frequency is separated from the other, the less chance of the fading. Frequency diversity has many disadvantages, such the requirement of additional power to transmit the signal over multiple frequency bands. But the main disadvantage of the frequency diversity is that it requires higher amount of frequency spectrum in order to send many copies of the signal, which is a loss of radio resources, and a decrease in the data rate. instead, parts of the signal can be carried over different frequency components (i.e. spread it over a large bandwidth). This spreading can be done by multi carrier modulation and frequency hopping [14].

**Path Diversity:** As multi path signals pass through different paths, they are all the time shifted in relation to each other. Thus, this technique is efficient if the signal bandwidth is much larger than the channel coherence bandwidth. And the multi path components are better exploit when they are resolvable and non-overlapping, so the signal can be uncorrelated [14].

## 3.2 MIMO SYSTEMS

Communications over radio systems have standards for the number of antennas, i.e. input and output signals. Starting with a standard Single Input Single Output (SISO) implementation, we can create transmit diversity by using multiple antennas at the transmitter, this configuration is called Multiple Input Single Output (MISO). Similarly, we can add receive diversity by using multiple antennas at the receiver and we get a configuration called

Single Input Multiple Output (SIMO). Real MIMO starts when multiple antennas are used at both the transmitter and the receiver. SISO systems are used in all wired communication systems beside many wireless communication systems. While the other two systems are mostly exclusive in radio transmission.

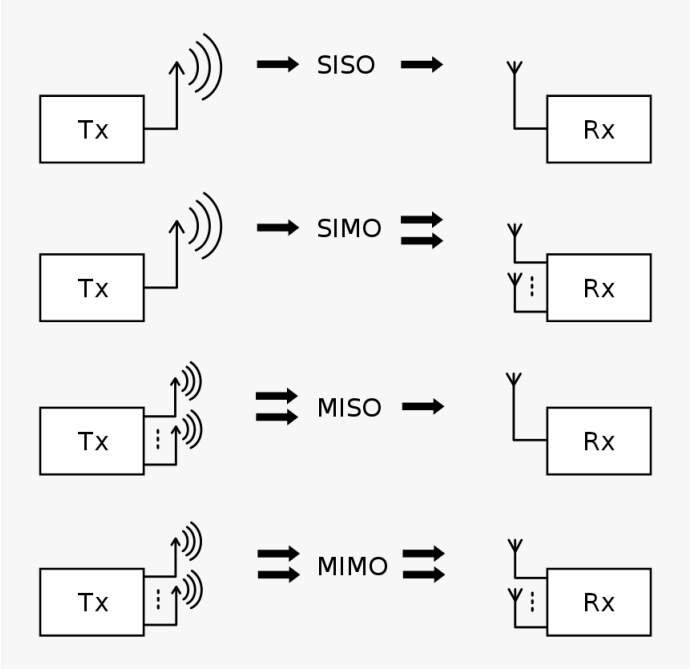


**Figure 3.3:** SISO SIMO MISO MIMO

Better transmission results can be obtained by implementing more antennas, but this leads us to many restrictions such as the cost, the need for space and processing power to handle the multiple streams of data [14][40].

### 3.2.1 Multiple Antennas

MIMO technology has attracted much attention in wireless communications, because it offers significant increases in data throughput and link range without an additional increase in bandwidth or transmit power. These technologies offer significant advantages over a single antenna system, and improve reliability in fading environments and higher data. Furthermore, channel capacity of a multi-antenna system is increased as compared to conventional single antenna systems, without any additional transmit power or spectral bandwidth.

### *MIMO Propagation Model*

In contrast to traditional communication systems with one transmit and one receive antenna, MIMO systems are equipped with multiple antennas at both transmission sides. Therefore, it is needed to describe all transmit and receive antenna pairs in the MIMO channel [18]. Consider $N_{tx} \times N_{rx}$ MIMO systems with $N_{tx}$ transmit and $N_{rx}$ receive antennas, as shown in figure 3.4 [41]:

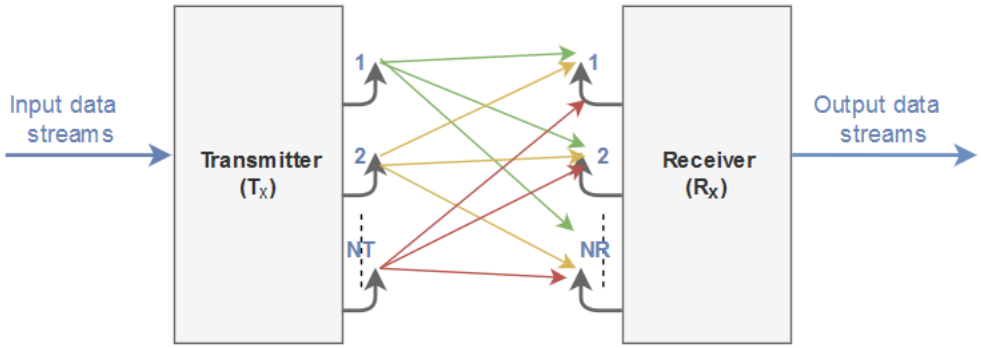


**Figure 3.4:** MIMO channel

From a system level viewpoint, a linear time-variant MIMO channel is represented by an $N_{tx} \times N_{rx}$ channel matrix.

$$H(t,\tau) = \begin{pmatrix} h_{11}(\tau,t) & h_{12}(\tau,t) & \cdots & h_{1NR}(\tau,t) \\ h_{21}(\tau,t) & h_{22}(\tau,t) & \cdots & h_{2NR}(\tau,t) \\ \vdots & \vdots & \ddots & \vdots \\ h_{NT1}(\tau,t) & h_{NT2}(\tau,t) & \cdots & h_{NTNR}(\tau,t) \end{pmatrix} \tag{3.1}$$

Where $h_{ij}(\tau,t)$ is the impulse response of the channel between the $j^{th}$ transmitter element and the $i^{th}$ receiver element. Those elements are complex numbers, and their distribution corresponds to the physical propagation environment of the wireless channel, and is the delay of the received signal [41][42].

The over-all MIMO input-output relation between the transmit signal vector of length-m and the receive signal vector of length-n can be formulated as [41]:

$$y(t) = \int_{\tau} H(t,\tau)s(t-\tau)d\tau + n(t) \tag{3.2}$$

$n(t)$ denotes noise and interference. If the channel is constant over time, the channel matrix dependence on $t$ disappears, and considering a narrow bandwidth where the channel is frequency-invariant, then the corresponding input-output relationship in (3.2) simplifies to as [42]:

$$y(t) = \int_{\tau} Hs(t) + n(t) \tag{3.3}$$

The elements of the MIMO channel matrix **H** are not always independent, because of the insufficient antenna elements spacing and the limited environmental scattering [43].

***Benefits of MIMO Systems***

MIMO systems take advantages of the transmit and receive multi-antenna benefits simultaneously but they also offer new advantages compared to conventional antenna array systems [44]:

**Array Gain:** Compared to the conventional SISO systems, array gain indicates improvement of Signal to Noise Ratio (SNR) at the receiver. These improvements can be due to the coherent combining of multiple signals with correct processing, either from multiple transmitters or from multiple receivers. It is necessary that the Channel State Information (CSI) has to be known at the transmit side in order to achieve array gain at the transmitter antenna array. On the other hand, the channel has to be known at the receive side for the exploitation of antenna array gain at the receiver. Receive array gain is achieved regardless of the correlation between the antennas.

**Diversity Gain:** In wireless communications, diversity is important to overcome fading. The more independent fading channels exist, the less probability of deep fading occurs. Although there are many fading techniques, but they are all based on the same principle: transmitting the signal through several independent fading paths. The most well known and widely used types of diversity in the wireless communications are: time diversity, frequency diversity, and space diversity. Measurements have shown that as regards the base station, the height of the base station and the coherence distance are strongly correlated: higher are the base station antennas, larger is the coherence distance.

**Multiplexing Gain:** Several antennas at both ends of the communication system is needed to exploit multiplexing gain. In the MIMO system with rich scattering environment, several communication channels in the same frequency band can be used. It was proven that the capacity of the spatial multiplexing system can be increased with the minimum number of transmit and receive antennas. Such increase in spectral efficiency of the system is very attractive since there is no need for additional spectrum or for increasing transmit power.

### 3.2.2 Massive MIMO

Recently MIMO technology has been studied and applied to many wireless standards since it can substantially improve the capacity and reliability of wireless systems. Initial work focused on point-to-point MIMO links where two devices with multiple antennas communicate with each other, but later on, effort were investigated to obtain more dramatic gains and simplify the required signal processing, leading to propose massive MIMO systems or large-scale antenna systems, which basically refers to the system where hundreds of antennas simultaneously serve dozens of user terminals in the same time-frequency resource.
The basic premise behind mMIMO is to reap all the benefits of conventional MIMO, but

on a much greater scale. Therefore, focus has shifted in the latest years to more practical multi-user MIMO systems where each base station (BS) is typically equipped with multiple antennas e.g., 100 or more, this BS serves a group of single-antenna users at the same time. Furthermore, the need of expensive equipment will be required just in BS end of the link, while relatively cheap single-antenna devices can be implemented at the user terminal [45]. A massive MU-MIMO network is illustrated in figure 3.5:

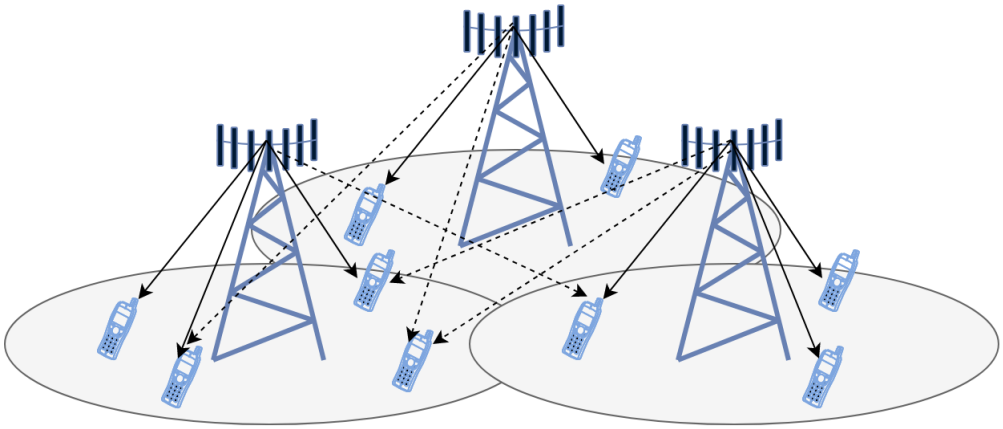

**Figure 3.5:** mMIMO

Due to multi-user diversity, the performance of MU-MIMO systems is generally less sensitive to the propagation environment than in the point-to-point MIMO case [45]. It improves the bandwidth efficiency substantially, since it can achieve large multiplexing gains when serving tens of user equipments simultaneously, which leads to reducing the transmit power [46]. On the other hand, it improves the energy efficiency due to the fact that using a large number of antennas helps focus energy with an extremely sharpness narrow beam into small regions in space where the User Terminal (UT)s are located [46][47].

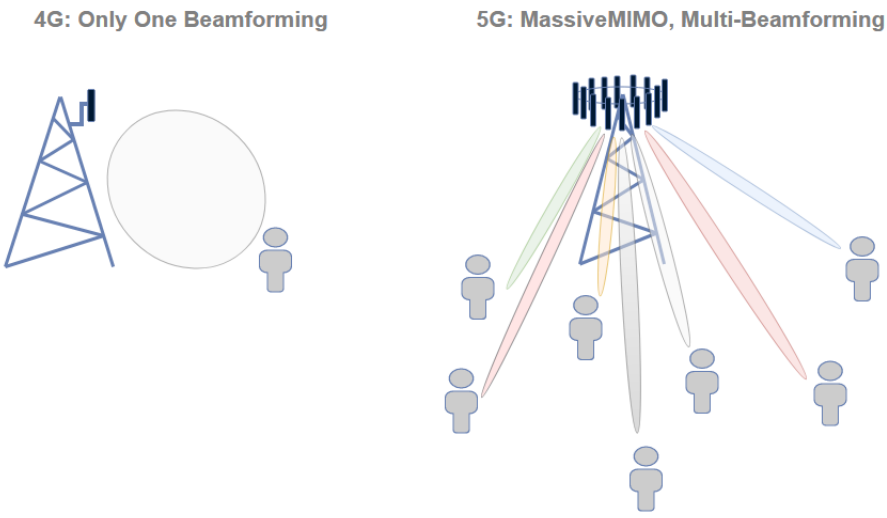


**Figure 3.6:** Beamforming difference between MIMO and mMIMO

Another characteristic of mMIMO system is that the number of antennas is assumed to be much greater than the number of users, this offer extra freedom to design the shape of the transmitted signals in a hardware-friendly way [48]. A mMIMO system has a large surplus of degrees of freedom. For example, with 200 antennas serving 20 terminals, 180 degrees of freedom are unused. These degrees of freedom can be used for hardware-friendly signal shaping. In particular, each antenna can transmit signals with very small PAPR [49] or even constant envelope [50] at a very modest penalty in terms of increased total radiated power [46].

- mMIMO can be built with less inexpensive and less power consuming components. It is a game changing technology regarding theory, systems, and implementation. With mMIMO, the expensive ultra-linear amplifiers that are used in conventional systems with output power of around 50 W are replaced by hundred mill-Watt range amplifiers. The contrast to classical array designs, which use few antennas fed from high-power amplifiers, is significant. Many high cost and bulky items, like large coaxial cables, can be eliminated.
- mMIMO reduces the accuracy and linearity limitations of each single amplifier and RF chain. Their combined action is the most important principle. When signals from a large number of antennas are combined in the air, mMIMO ensures that noise, fading, and hardware imperfections average are significantly reduced depending on the law of large number of antennas. The same feature that makes mMIMO resists fading makes the technology extremely robust to failure of one or a few of the antenna unit(s).
- mMIMO enables a huge reduce in latency on the air interface. The performance of wireless communications systems is strongly affected by fading that can render the received signal strength very small. At certain times, when the transmitted signal from a base station travels through multiple paths it suffers from destructive interference before it reaches the terminal. It is what makes it hard to build low-latency wireless links. If the terminal is trapped in a fading dip, the data cannot be received again until the propagation channel is sufficiently changed.

In order to avoid fading dips, mMIMO relies on the law of large numbers and beamforming so fading no longer limits latency. In fact asymptotic arguments based on random matrix theory denotes that as the number of antennas in a MIMO cell grows to infinity, the transmitted power required for each bit will be eliminated. Hence, the effects of uncorrelated noise and small-scale fading disappear. In addition, the use of simple linear signal processing approaches, such as Matched Filter (MF) precoding/detection, can be used in massive MIMO systems to fulfill these advantages [44][46].

### 3.2.3 Antenna Configurations

In general, there are strong evidences that the most appropriate propagation assumptions for massive mMIMO system are valid in practice [51]. It strongly depends on the configuration and deployment of the antenna arrays which in turn critically affect the channel properties assigning different mMIMO performances. Hence, there are several practical issues regarding the implementation of the antenna arrays. Figure 3.7 illustrates several typical antenna configurations namely the linear Antenna Array (AA), spherical AA, cylindrical AA, rectangular AA, and distributed AA . The linear AA is an example of Two-Dimensional (2D) AAs that is mostly assumed in theoretical analysis and realistic measurements [24]. Whereas the spherical AA, cylindrical AA and rectangular AAs belong to the family of Three-Dimensional (3D) AAs. Considering the space limitations at both the transmission sides, the spherical, cylindrical and rectangular AAs are more realistic for practical systems. With these arrays we can adjust both azimuth and elevation angles, and propagate signals in 3D space that are more realistic for practical systems. The distributed AA is mainly used either inside buildings or for outdoor cooperation, Each of those configurations as well as their size affects the channel properties assigning different mMIMO performances. For example, the distance between the antenna elements basically dictates mutual coupling and the correlation matrix, affecting the performance of mMIMO [52]. One of the major constrains of applying mMIMO is the large size of the AA , therefore, it is important to select a proper AA configuration. Some solutions were proposed, such in [53] the use of distributed AA was proposed, it provides an implementation of great number of antennas in the same space.

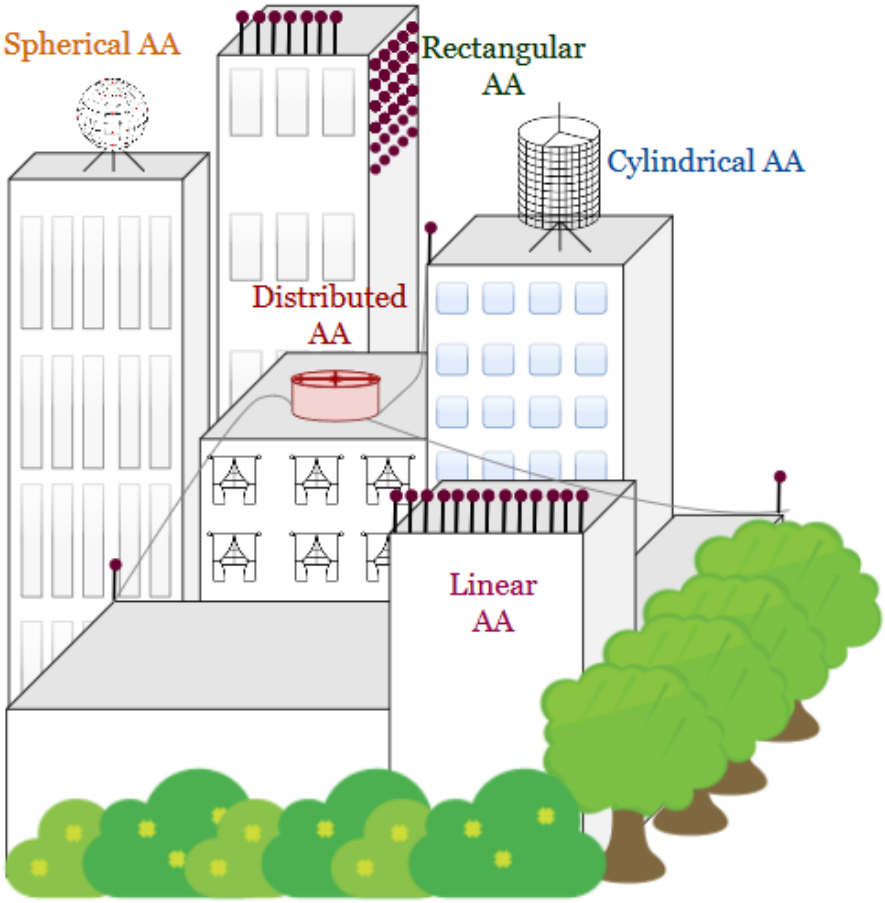


**Figure 3.7:** Antenna configuration

### 3.2.4 Massive MIMO in the context of millimeter-wave systems

mmWave communications 30-300 GHz where the spectrum is less crowded and wider bandwidths are available, is considered among the best candidates to provide multi-gigabit communication services and wideband multimedia applications, it plays a pivotal role in the future mobile internet, such as, vehicular network, virtual and augmented reality. In other words, access communications that can provide up to 10,000x capacity over today's systems, and which will be required by 2030, seems to be feasible.

Furthermore, the characteristics of radio wave propagation vary from one frequency band to another. If we compare mmWave to signals at lower frequencies, we find that the large bandwidth available at the mmWave frequency band provides much greater capacity than the current sub-6 GHz alternatives. However, mmWave are more susceptible to path-loss, reflection loss and it cannot propagate well through most materials which results mmWave channels being weak and sparse scattering [54]. In [55] some of the major mmWave propagation characteristics were described:

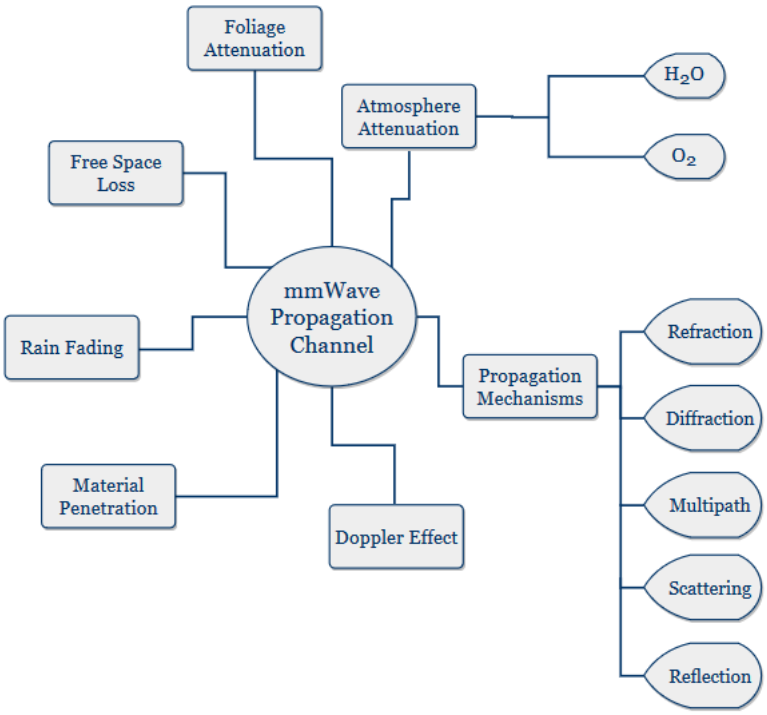


**Figure 3.8:** mmWave propagation characteristics

1. **Free-Space Loss:** Free-Space Loss (FSL) is proportional to separation distance and carrier frequency. Hence, using a carrier of mmWave frequency band, means high FSL.
2. **Rain-Induced Fading:** mmWave signals are more likely to be blocked by raindrops than signals with longer wavelengths due to their small size. The interaction between the propagating waves and the rain droplets at mmWave causes attenuation.
3. **Atmospheric Attenuation:**This factor is the atmospheric attenuation caused by gas molecules in the Earth's atmosphere. The atmospheric attenuation is caused by the vibrating nature of air molecules when exposed to radio waves. Molecules absorb a certain portion of the radio wave's energy and vibrate with a strength proportional to the carrier frequency.

## 3.3 MIMO CHANNEL MODELS

The need for different spatial channel models has been revealed in conjunction with the existence of MIMO wireless systems. Channel models are used to provide the accurate predictions of a channel performance in a specific environment. Hence, MIMO channel models can be classified regarding the difference in channel properties with respect to time. In fact, there are two types: statistical models and physical models. Statistical models are simpler but less accurate, they basically rely on practical statistics valid for a given environment. Oppositely, the physical models are more accurate, but are based on some physical parameters that depend on the considered scenario and the computation can be more complex [41].
Many spatial channel models were developed to characterize the MIMO impulse response.

A classification of the MIMO channel model is summarized in figure 3.9. They are mainly categorized as Deterministic, stochastic and hybrid models [56] [57].

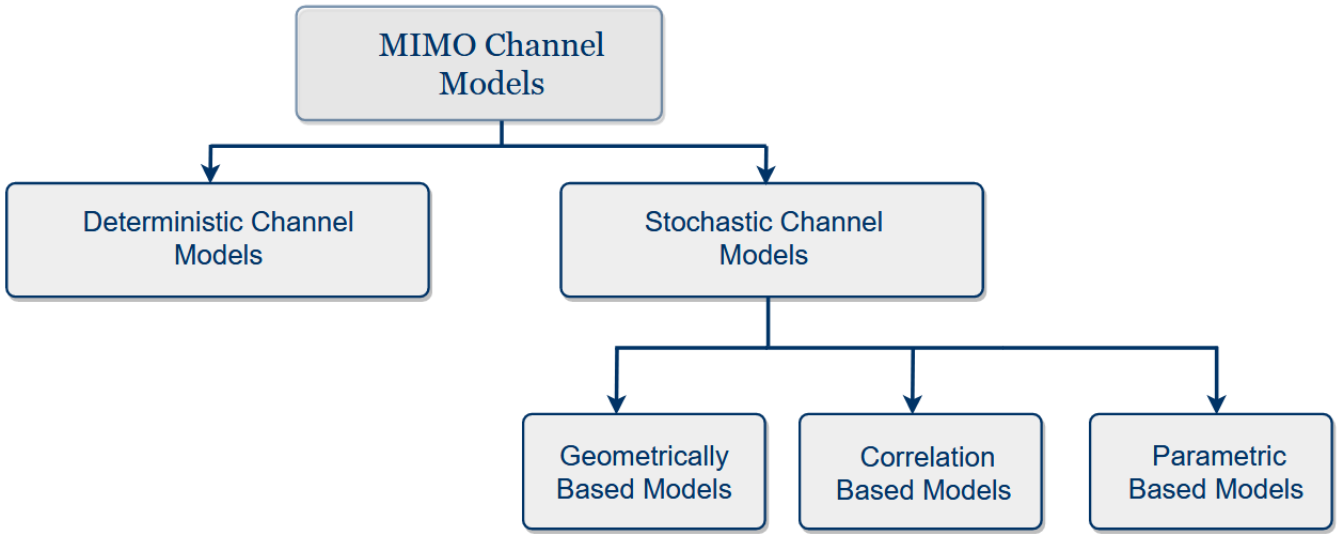


**Figure 3.9:** Classification of MIMO channel models

- **Deterministic Channel Models:**
  Deterministic channel models are those models that gives the specification of the environment is given specifically. It can also be called field measurements that clearly define information regarding the potential performance of a particular propagation environment. This channel modelling does not consider the antenna as the part of channel. In other words, deterministic channel models are mostly site specific models not general models.

- **Stochastic Channel Models:**
  Stochastic channel model is used to estimate the probability distributions of potential outcomes. It allows random time variation in one or more inputs based on the observed fluctuations in historical data, using standard time-series techniques.

  1. *Geometrically Based Models:*
     Geometric channel models are based on the concept of scattering within the propagation environment. In this model stochastic distribution of the scattering around the transmitter and receiver is assumed. In order to provide a precise model of the channel, it requires a sufficient idea about the location of the spatial scatterer density function. Therefore, this model is considered less accurate than the deterministic models. On the other hand, it is faster in computation and has

less complexity. In addition to being adaptable to all environmental configurations.

2. *Correlation Based Models:*
   Correlation based channel model is not categorized as a physical channel. It basically exploits the various correlation characterizations of channels like space, time and frequency correlation between transmit and receive antennas. By the help of various correlation matrices derived from the assumptions about the antenna types and array configurations, correlation functions can be derived and provide detail of channel model. The main drawback of this channel model is the limited flexibility.

3. *Parametric Based Models:*
   In order to simplify the operations in these models, antenna characteristics are not usually considered. Parametric channel models are mainly divided into geometric and non-geometric based channels. An example of a non-geometric parametric channel model is Saleh-Valenzuela channel model.

### 3.3.1 Saleh–Valenzuela Model

The Saleh–Valenzuela model essentially describes the stochastic properties of the arrival delays and amplitudes of resolvable MPCs in WB wireless transmission systems. Based on the multipath rays arriving to the receiver in groups called clusters, formed by the multiple reflections from the objects in the vicinity of receiver and transmitter. Each ray and cluster have independent fading and arrive according to Poisson processes with different rates. The later the rays and clusters arrive, the lower is their power [58][59].
The Saleh-Valenzuela channel model can be expressed as [22],

$$h(t) = \sum_{c=0}^{+\infty} \sum_{r=0}^{+\infty} \beta_{c,r} e^{j\phi_{c,r}} \delta(t - T_c - \tau_{c,r}), \tag{3.4}$$

where $\beta_{c,r}$ is the arrival amplitude of $r$th ray from $c$th cluster, with Rayleigh distribution and conditional mean square values where the average power is $\overline{\beta_{c,r}^2} = \overline{\beta_{0.0}^2} e^{-\frac{T_c}{\Gamma}} e^{-\frac{\tau_{c,r}}{\gamma}}$, being $\beta_{0.0}^2$ the average power of 1st ray from 1st cluster, that depends of distance between transmitter and receiver. $T_c$ is the arrival delay of $c$th cluster and $\tau_{c,r}$ is the arrival delay of $r$th ray in the cluster. The phase $\phi_{c,r}$ is a random variable uniformly distributed in $[0, 2\pi]$. Finally, $\Gamma$ and $\gamma$ are the cluster and ray decay factor, respectively.

Figure 3.10 illustrates the idea, where the first cluster corresponds the received direct-path component and multi path components caused by the scatters around the transmitter and receiver. The average cluster and ray decays are represented by blue and red lines, that depends of this factors, $\Gamma$ and $\gamma$.

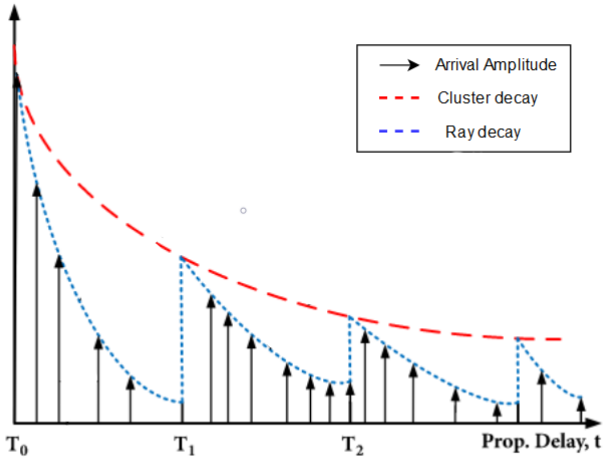


**Figure 3.10:** Saleh-Valenzuela channel response [60]

### 3.3.2 Wideband Channel Model

The combination between high levels of antenna correlation and the limited spatial selectivity or scattering caused by the characteristic of mmWave propagation and transceivers, makes the conventional statistical fading distributions inappropriate for mmWave channel modeling. Theretofore, several sparse channel models have been proposed for mmWave communications, one of them is the clustered channel model derived from the extended Saleh-Valenzuela channel model. A WB channel model $\mathbf{H}_{u,d}$ represents the sum of the contribution of each $N_{cl}$ cluster with $N_{ray}$ propagation path. Hence it is considered as a clustered channel [61], where the delay$-d$ MIMO channel matrix of the $u$th user denoted by $\mathbf{H}_{u,d} \in \mathbb{C}^{N_{rx} \times N_{tx}}$, can be given by

$$\mathbf{H}_{u,d} = \sqrt{\frac{N_{rx}N_{tx}}{\rho_{PL}}} \sum_{q=1}^{N_{cl}} \sum_{l=1}^{N_{ray}} \left(\alpha_{q,l}^{u} p_{rc}(dT_s - \tau_q^u - \tau_{q,l}^u)\, \mathbf{a}_{rx,u}\left(\phi_{q,l}^{rx,u}, \theta_{q,l}^{rx,u}\right) \mathbf{a}_{tx,u}\left(\phi_{q,l}^{tx,u}, \theta_{q,l}^{tx,u}\right)^H, \tag{3.5}$$

where $\rho_{PL}$ represents the path-loss between the transmitter and the receiver, $\alpha_{q,l}^u$ is the complex path gain of the $l$th ray in the $q$th scattering cluster, and for the pulse shaping function $p_{rc}(.)$ a raised-cosine filter is used. The $q$th cluster has a time delay $\tau_q^u$ while each ray $l$ from $q$th cluster has a relative time delay $\tau_{q,l}^u$ and the path delay is uniformly distributed in $[0, DT_s]$ , where $D$ is the cyclic prefix length and $T_S$ is the sampling interval. The angles $\phi_{q,l}^{rx,u}$ , $\theta_{q,l}^{rx,u}$ , $\phi_{q,l}^{tx,u}$ , and $\theta_{q,l}^{tx,u}$ are the azimuth and elevation angles of arrival and departure, respectively. $\phi_{q,l}^{rx,u}$ has a Laplacian distribution with mean $\phi_q^{rx,u}$ uniformly distributed in $[0, 2\pi]$ and variance $\sigma^2_{\phi_q^{rx,u}}$ . The remaining angles have similar distributions.
For a Uniform Linear Array (ULA) on the y-axis, with $N_y$ elements, the array response vector is given by

$$\mathbf{a}_{ULA}(\phi) = \frac{1}{\sqrt{N_y}}\left[1, e^{j1kd\sin(\phi)}, e^{j2kd\sin(\phi)}, ..., e^{j(N_y-1)kd\sin(\phi)}\right]^T, \tag{3.6}$$

where $k = 2\pi/\lambda$, $\lambda$ is the wavelength, $d$ is the inter-element spacing. Therefore, from (3.5), the channel $\mathbf{H}_{u,k} \in \mathbb{C}^{N_{rx} \times N_{tx}}$ of the $u$th user at the sub-carrier $k$ can be represented as

$$\mathbf{H}_{u,k} = \sum_{d=0}^{D-1} \mathbf{H}_{u,d} e^{-j\frac{2\pi k}{N_c} d}, \tag{3.7}$$

(3.7) can also be expressed as

$$\mathbf{H}_{u,k} = \mathbf{A}_{rx,u} \Delta_{u,k} \mathbf{A}_{tx,u}^{H}, \tag{3.8}$$

where $\Delta_{u,k}$ is a diagonal matrix, with entries $(q, l)$ that correspond to the paths gain of the $l$th ray in the $q$th scattering cluster.
$\mathbf{A}_{tx,u} = [\mathbf{a}_{tx,u}(\phi_{1,1}^{tx,u}, \theta_{1,1}^{tx,u}), \ldots, \mathbf{a}_{tx,u}(\phi_{N_{cl},N_{ray}}^{tx,u}, \theta_{N_{cl},N_{ray}}^{tx,u})]$
and $\mathbf{A}_{rx,u} = [\mathbf{a}_{rx,u}(\phi_{1,1}^{rx,u}, \theta_{1,1}^{rx,u}), \ldots, \mathbf{a}_{rx,u}(\phi_{N_{cl},N_{ray}}^{rx,u}, \theta_{N_{cl},N_{ray}}^{rx,u}))]$ hold the transmit and receive array response vectors of the $u$th user, respectively.

## 3.4 HYBRID ARCHITECTURE

Large antenna arrays will be intensively used in the future mmWave cellular networks. Hence, different possible antenna architectures and MIMO techniques will be needed. These challenges instigate the expanding of communications theory where mmWave mMIMO systems demand the pack of a large number of antennas into a small form factor. In typical digital systems, a distinct RF chain is required for each antenna element at the receiver side, which naturally will put prohibitive burdens on cost and power consumption, especially for mobile terminals, and thus is not feasible. On the other hand, because of the constraints of using mmWave bandwidth (mainly the path loss as mentioned previously), effective beamforming becomes crucial to combat the restrictions and exploit the abundant mmWave spectrum [62][63].

An RF chain includes low-noise amplifier, down-converter, Digital to Analog Converter (DAC), Analog to Digital Converter (ADC) and so on [62] implies that a large number of hardware components will be needed to support conventional digital beamforming. Therefore, the high cost and power consumption of those mixed signal components, such high-resolution ADCs, makes it difficult to dedicate a separate complete RF chain with these components for each antenna. In hybrid analog/digital architectures, as we can find in figure 3.11, some signal processing is done at the digital domain and some left to the analog domain, in fact transmitters have the ability to apply high-dimensional RF precoders relying on phase shifters, followed by low-dimensional digital precoders that can be implemented at baseband [64].

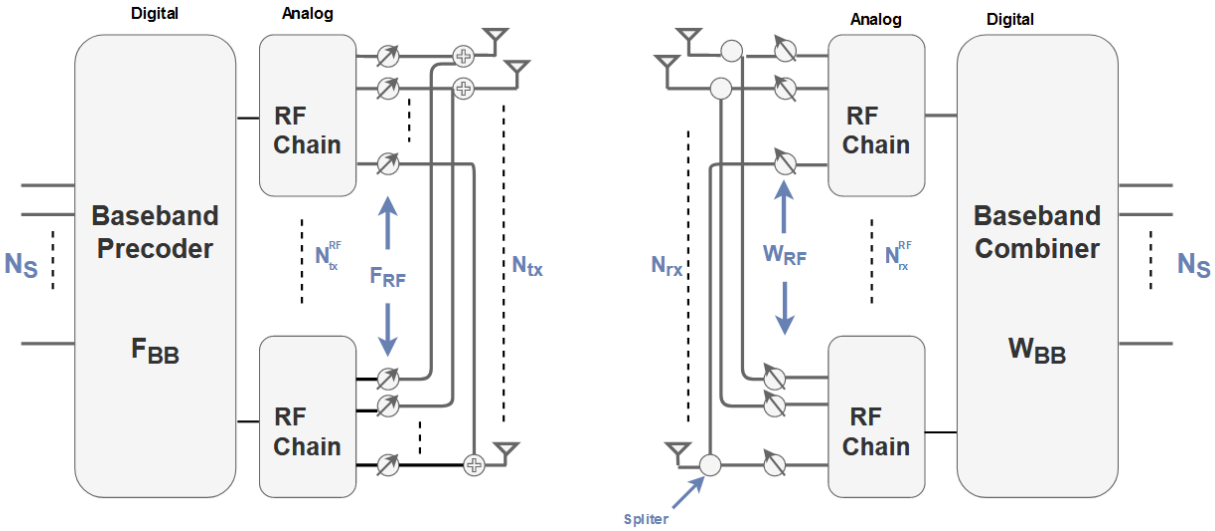


**Figure 3.11:** Hybrid Architecture

Hybrid structures can be mainly divided into full-connected and sub-connected hybrid analog-digital architectures, the main difference between the two schemes is illustrated in figure 3.12.
In a fully connected hybrid beamforming structure, each RF chain is connected with all antennas, and the transmitted signal on each of the $N_{tx}$ digital transmitters goes through $N_{tx}^{RF}$ paths (mixer, power amplifier, phase shifter, etc.) and summed up before being connected with each antenna. The fully-connected structure provides full beamforming gain per transceiver but has a high complexity, e.i. the number of phase shifters required for a fully connected structure is $N_{tx} \times N_{tx}^{RF}$. Where $N_{rx}$ and $N_{rx}^{RF}$ are the number of antennas and the number of RF chains [65].

In sub-connected structure, each antenna is connected with only $T = N_{tx}/N_{tx}^{RF}$ antennas. Thus, sub-connected architecture has lower hardware complexity of $N_{RF}^{tx}$ paths at the cost of $1/N_{tx}^{RF}$ beamforming gain compared with fully-connected structure. Thus, the power consumption used to excite and to compensate the insertion loss of phase shifters is reduced, and the computational complexity is lower [62].

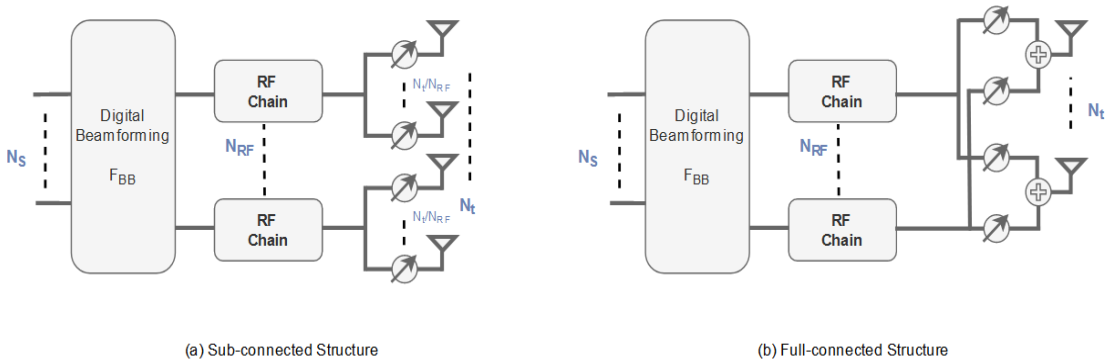


**Figure 3.12:** Full-connected and Sub-connected Hybrid Architecture

CHAPTER 4

# Design and Implementation of Hybrid Equalizer for mmWave mMIMO GFDM Systems

*This chapter presents the proposed full-connected hybrid system, where a hybrid multiuser equalizer combined with low complexity hybrid precoder for WB mmWave mMIMO systems is implemented. A full-digital GFDM modulation technology is considered as a modulation scheme. For the transmitter, two analog precoding methods are described and for the receiver, a hybrid analog-digital equalization method is presented. Finally, the proposed schemes are assessed under the mmWave broadband channel model discussed in chapter 3.*

## 4.1 SYSTEM MODEL

This work considers a multi-user mmWave massive MIMO system with an hybrid analog-digital architecture at both the transmitter and receiver. For the access technique the GFDM modulation scheme was considered. The transmitter side has $N_{tx}$ transmitting antenna with a single RF chain, while at the receiver side the number of RF chains $N_{rx}^{RF}$ is lower/equal to the number of the receiving antennas $N_{rx}$, i.e., $U \leqslant N_{rx}^{RF} \leqslant N_{rx}$. Each GFDM block contains $K$ subcarriers with $M$ symbols on each subcarrier, and $N = KL$ samples per symbol, where $L$ denotes the oversampling factor. We consider $U$ user terminals in the same radio recource sending one data stream per subcarrier.

### 4.1.1 Transmitter

At the transmitter, the proposed hybrid multiuser equalizer mmWave mMIMO based systems is mainly divided into two major parts: the analog part represented by analog precoding procedure, and the digital part where a GFDM modulation is applied.

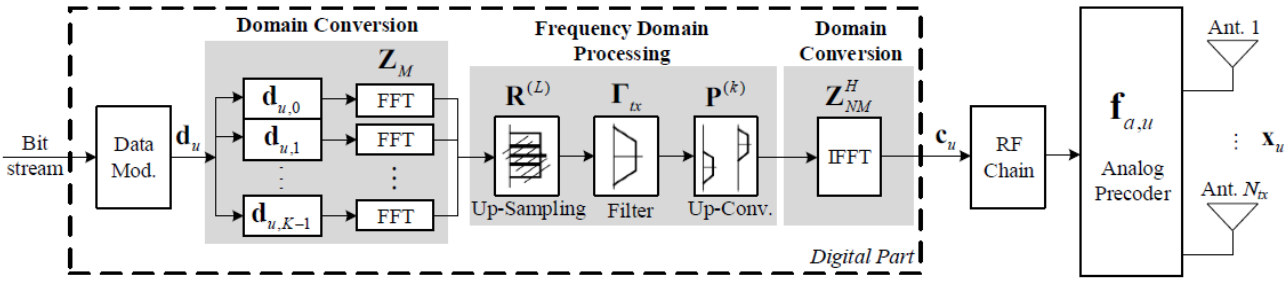


**Figure 4.1:** Block diagram of the transmitter

*The Digital Part*

Figure 4.1 illustrates the modulation procedure done at the UT. After generating a bit stream $\mathbf{d}_u = [d_{u,0}, d_{u,1}, \ldots, d_{u,KM-1}]^T \in \mathbb{C}^{KM}$ and modulating it by M-ary Quadrature Amplitude Modulation (MQAM) constellation, this stream is divided into $K$ sequences, $\mathbf{d}_{u,k} = \{d_{u,l}\}_{l=kM}^{(k+1)M} \in \mathbb{C}^M$, which are spread on $k = 0, \ldots K-1$ sub-carriers and $m = 0, \ldots M-1$ time slots, respectively. Hence, we get the data matrix $\mathbf{D}$ , in which each row refers to a time slot and each column refers to a sub-carrier.

Then, the converting process from time to frequency domain is shown in the domain conversion block where a DFT matrix $\mathbf{Z}_M \in \mathbb{C}^{M \times M}$ is applied, given by

$$\mathbf{Z}_M = \frac{1}{\sqrt{M}} e^{-j2\pi \frac{kn}{N}}, \quad n = 0, ..., N-1, \tag{4.1}$$

From here we get the vector $\mathbf{Z}_M \mathbf{d}_{u,k}$ for each $\mathbf{d}_{u,k}$, which represent the data at sub-carrier $k$ in the frequency domain, the domain all the processing takes place [66], then it passes through the block of frequency processing that contains three operations corresponding to the three blocks in figure 4.1. Each stage may be represented by a matrix and thus, the signal at the output of each block is equal to the signal at the input multiplied by the corresponding matrix.

The first one is the up-scaling process where the output vector of the domain conversion block is multiplied by the repetition matrix

$$\mathbf{R}^{(L)} = \underbrace{[\mathbf{I}_M, ..., \mathbf{I}_M]}_{L}^{T} \in \mathbb{C}^{LM \times M}, \tag{4.2}$$

to reproduce the samples $L$ times, where $\mathbf{I}_M$ is an identity matrix, therefore we get $\mathbf{R}^{(L)} \mathbf{Z}_M \mathbf{d}_{u,k}$, then it passes through the filtering block, where we apply a pulse shaping filter matrix $\mathbf{\Gamma} = \text{diag}(\mathbf{Z}_{LM}\mathbf{g}) \in \mathbb{C}^{LM \times LM}$ to each sub-carrier, this matrix contains frequency samples $\mathbf{g}$ on its diagonal and zeros otherwise. In the last block in the frequency domain processing, a circular up-converting process is applied on $k$th sub-carrier signal to up-convert it from base-band to band-pass by a multiplication with a permutation matrix $\mathbf{P}^{(k)} \in \mathbb{C}^{NM \times LM}$, where $\mathbf{P}^{(1)} = [\mathbf{I}_{LM}, \mathbf{0}_{LM}, \mathbf{0}_{LM}, ...]^T$,$\mathbf{P}^{(2)} = [\mathbf{0}_{LM}, \mathbf{I}_{LM}, \mathbf{0}_{LM}, ...]^T$,.. with $0_{LM}$ square matrix

that contains zero elements [66]. Then again, the signal is transformed back to time domain, which is the domain necessary for transmission by applying $NM$ point IDFT matrix $\mathbf{Z}_{NM}^{\mathrm{H}}$ on the sub-carriers so all sub-carriers signal are superimposed $\mathbf{c}_u = [c_{u,0}, ..., c_{u,NM-1}]^T \in \mathbb{C}^{NM}$, and transformed to the time domain

$$\mathbf{c}_u = \mathbf{Z}_{NM}^H \sum_{k=0}^{K-1} \left( \mathbf{P}^{(k)} \mathbf{\Gamma}_{tx} \mathbf{R}^{(L)} \mathbf{Z}_M \mathbf{d}_{u,k} \right) \tag{4.3}$$

As a matter of the fact that GFDM modulation procedure at the transmitter side is usually presented by a matrix, we can simplify the previous equation in order to facilitate the application of standard receiver methods such as MF, Zero Forcing (ZF), and Minimum Mean Square Error (MMSE). Hence, (4.3) can be reformulated as:

$$\mathbf{c}_u = \mathbf{Z}_{NM}^H \mathbf{A} \mathbf{d}_u, \tag{4.4}$$

where $\mathbf{A} = [\mathbf{A}_0, \mathbf{A}_1, \ldots, \mathbf{A}_{K-1}] \in \mathbb{C}^{NM \times KM}$ is the complex-valued modulation matrix that contains all transmitted signals as $\mathbf{A}_k = \mathbf{P}^{(k)} \mathbf{\Gamma} \mathbf{R}^{(L)} \mathbf{Z}_M \in \mathbb{C}^{NM \times M}$.
At this stage, the digital process is completed, and the data is passed to the analog phase, where the analog precoder $\mathbf{f}_{a,u} \in \mathbb{C}^{N_{tx}}$ is applied on $\mathbf{c_u}$ to obtain the transmitted signal $\mathbf{x}_{u,l} \in \mathbb{C}^{N_{tx}}$ :

$$\mathbf{x}_{u,l} = \mathbf{f}_{a,u} c_{u,l} \ , \ l = 0, ...NM - 1. \tag{4.5}$$

*The Analog Part*

The precoder in the first place is built of analog phase shifters[67]–[69] with constant amplitude, that forces all vector elements of $\mathbf{f}_{a,u} \in \mathbb{C}^{N_{tx}}$of the matrix $\mathbf{F}_{a,u}$ to have the same magnitude ($|\mathbf{f}_{a,u}(n)|^2 = N_{tx}^{-1}$).
The precoder performance in this work depends on CSI knowledge at the user terminal [70]. The precoder can be computed based on the knowledge of the channel by judicious weighting of the signals from each antenna. [71]. As mentioned in chapter 3, channel estimation for the uplink can be done by sending different pilot sequences from the users to the BS.[45] We consider two hybrid analog-digital precoders depending on the levels of CSI knowledge at the UTs:

1. **No CSI at User Terminals** In this case, we assume that the UT has no access to CSI and the analog precoder vector is generated randomly for the $u$th user according to [72]:

   $$\mathbf{F}_{a,u} = [e^{j2\pi\phi_n^u}]_{1 \leqslant n \leqslant N_{tx}} \tag{4.6}$$

   where $\phi_n^u$, $n \in \{1, \ldots, N_{tx}\}$ , and $u \in \{1, \ldots, U\}$ are i.i.d. uniform random variables such that $\phi_n^u \in [0, 1]$.

2. **Partial CSI at User Terminals**
   In this case, designed in [48], we consider an analog precoder based on the knowledge of partial CSI at the transmitter, i.e., supposing that only the average Angles of

Departure (AoD) is known at the transmitter side. The main goal here is to maximize the power of the selected user, which in turn allows steering the beam in the dominant direction of the transmission channel. Considering the channel model presented in chapter 3. Foremost, we form the matrix :

$$\mathbf{A}_{tx,u} = [\mathbf{a}_{tx,u}(\phi_1^{tx,u}), ..., \mathbf{a}_{tx,u}(\phi_{N_{cl}}^{tx,u},)] \in \mathbb{C}^{N_{tx} \times N_{cl}}. \tag{4.7}$$

Afterward, we determine the eigenvalue decomposition of

$$\mathbf{A}_{tx,u}\mathbf{A}_{tx,u}^H = \mathbf{\Lambda}_{tx,u}\mathbf{\Sigma}_{tx,u}\mathbf{\Lambda}_{tx,u}^H.$$

Therefore, we move to select the dominant channel direction to use in the analog precoder, making

$$\mathbf{f}_{a,u}(n) = \frac{1}{\sqrt{N_{tx}}} \exp\{j \arg(\mathbf{\Lambda}_{tx,u}(n,1))\}, \quad n = 1, ..., N_{tx} \tag{4.8}$$

### 4.1.2 Receiver

Similar to the transmitter architecture, the signal in the receiver passes through two main parts, the analog part where the proposed analog equalizer is implemented for the sake of minimizing the mean square error between the hybrid approach and the full digital counterpart to efficiently separate the users that share the same radio resources. The digital part where GFDM demodulation is applied, separates the users and removes the remaining multiuser interference.

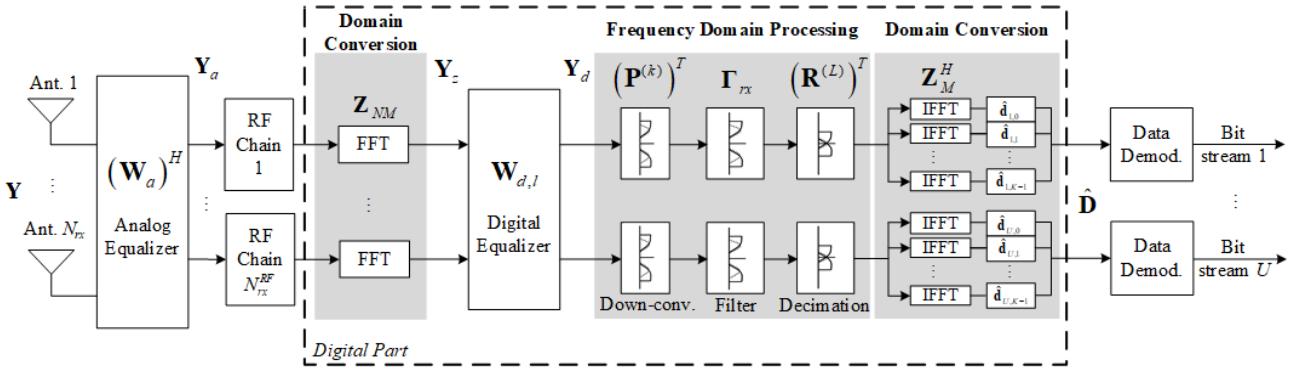


**Figure 4.2:** Block diagram of the receiver

Figure 4.2 illustrates the steps of the receiving process:
$\mathbf{x}_{u,l} \in \mathbb{C}^{N_{tx}}$ is the transmitted signal of the uth user and $\mathbf{y}_l$ is the received signal:

$$\mathbf{y}_l = \sum_{u=1}^{U} \mathbf{H}_{u,l}\mathbf{x}_{u,l} + \mathbf{n}_l \ = \mathbf{H}_l\mathbf{c}_l + \mathbf{n}_l, \ \ \mathbf{c}_l = [c_{1,l}, ..., c_{U,l}]^T \in \mathbb{C}^U \tag{4.9}$$

Where $\mathbf{n}_l \in \mathbb{C}^{N_{rx}}$ is a vector of Additive White Gaussian Noise (AWGN) that has zero mean variance $\mathbf{H}_l$ $\sigma_n^2$ and $\mathbf{H}_l$ is the channel

$$\mathbf{H}_l = [\mathbf{H}_{1,l}\mathbf{f}_{a,u}, ..., \mathbf{H}_{U,l}\mathbf{f}_{a,u}] \in \mathbb{C}^{N_{rx}\times U}. \tag{4.10}$$

The received signal is firstly processed through the analog phase shifters, modeled by the matrix $\mathbf{W}_a \in \mathbb{C}^{N_{rx}\times N_{rx}^{RF}}$. Each entry of $W_A$ corresponds to a phase shifter which are hardware components which only modify the phase of the input signal, therefore $|\mathbf{W_a}(i,j)|^2 = N_{rx}^{-1}$. The domain conversion block is firstly done in the digital part, then the digital equalizer is performed.

Starting with equation (4.4), we define :

$$\mathbf{C} = \mathbf{Z}_{NM}^H \mathbf{A}\mathbf{D}\,. \tag{4.11}$$

Where $\mathbf{D} = [\mathbf{d}_1, ..., \mathbf{d}_U] \in \mathbb{C}^{KM\times U}$ and $\mathbf{C} = [\mathbf{c}_1, ..., \mathbf{c}_U] \in \mathbb{C}^{NM\times U}$. Therefore, the received signal matrix, $\mathbf{Y} = [\mathbf{y}_0, ...\mathbf{y}_{NM-1}] \in \mathbb{C}^{N_{rx}\times NM}$ , is obtained from (4.9) and (4.10) by

$$\mathbf{Y} = \sum_{l=0}^{NM-1} \left( \mathbf{H}_l \mathbf{D}^T \mathbf{A}^T \left( \mathbf{Z}_{NM}^H \right)^T \mathbf{E}_{l+1} + \mathbf{N}\mathbf{E}_{l+1} \right) \tag{4.12}$$

where $\mathbf{N} = [\mathbf{n}_0, ...\mathbf{n}_{NM-1}] \in \mathbb{C}^{N_{rx}\times NM}$ and we can define $\mathbf{E}_l = \mathrm{diag}([0, 0, ..., 1, .., 0, 0]) \in \mathbb{C}^{NM\times NM}$ as a zero matrix, with the value 1 in position $l+1$ of diagonal.
From the equation (4.11) we can reformulate the equation (4.12) as

$$\mathbf{Y} = \sum_{l=0}^{NM-1} \left( \mathbf{H}_l \mathbf{C}^T \mathbf{E}_{l+1} + \mathbf{N}\mathbf{E}_{l+1} \right), \tag{4.13}$$

By applying the analog filter, we obtain

$$\mathbf{Y}_a = (\mathbf{W}_a)^H \mathbf{Y} = \sum_{l=0}^{NM-1} \left( (\mathbf{W}_a)^H \mathbf{H}_l \mathbf{C}^T \mathbf{E}_{l+1} + (\mathbf{W}_a)^H \mathbf{N}\mathbf{E}_{l+1} \right) \in \mathbb{C}^{N_{rx}^{RF}\times NM}, \tag{4.14}$$

Then we apply FFT on $\mathbf{Y}_z = \mathbf{Z}_{NM}\mathbf{Y}_a^T \in \mathbb{C}^{NM\times N_{rx}^{RF}}$ , so we get

$$\mathbf{Y}_z^T = \sum_{l=0}^{NM-1} \left( (\mathbf{W}_a)^H \mathbf{H}_l \mathbf{C}^T \mathbf{E}_{l+1} + (\mathbf{W}_a)^H \mathbf{N}\mathbf{E}_{l+1} \right) \mathbf{Z}_{NM}^T\,. \tag{4.15}$$

Consequently, the equalized receive signal formulation is

$$\mathbf{Y}_d = \sum_{l=0}^{NM-1} \left( \mathbf{W}_{d,l}(\mathbf{W}_a)^H \mathbf{H}_l \mathbf{C}^T \mathbf{E}_{l+1} + \mathbf{W}_{d,l}(\mathbf{W}_a)^H \mathbf{N}\mathbf{E}_{l+1} \right) \mathbf{Z}_{NM}^T \in \mathbb{C}^{U\times NM}. \tag{4.16}$$

From this point, we follow the frequency domain processing block as shown in figure 4.2, starting by the circular down conversion process depending on the transpose of the permutation matrix $\mathbf{P}^{(k)}$ , that combines two operations: circular down-conversion on the $k$th sub-carrier to zero frequency followed by removing frequency samples in the signal that correspond to

zero coefficients in the receive filter[73].
Then the receive filter $\mathbf{\Gamma}_{rx}^{(L)} = \left(\mathbf{\Gamma}_{tx}^{(L)}\right)^*$ is applied, noting that $\mathbf{\Gamma}_{rx}^{(L)}$ is the conjugated transmitter filter represented by $LM$ coefficients.
Afterwards, for the sake of producing $M$ samples that correlate with the transmitted data on the $k$th subcarrier, we use the matrix $(\mathbf{R}^{(L)})^T$ that correspond to the down-sampling process by a factor $L$ .

The last step is the time domain converting by applying matrix $\mathbf{Z}_M^H$ on the signal, and the de-mapping process to come by the estimation of the data bit constellation $\hat{\mathbf{D}} = [\hat{\mathbf{d}}_1, ..., \hat{\mathbf{d}}_U] \in \mathbb{C}^{KM \times U}$, where $\hat{\mathbf{d}}_u = [\hat{\mathbf{d}}_{u,0}^T, \hat{\mathbf{d}}_{u,1}^T, \ldots, \hat{\mathbf{d}}_{u,K-1}^T]^T \in \mathbb{C}^{KM}$ given by:

$$\hat{\mathbf{D}} = \mathbf{A}^H \mathbf{Y}_d^T. \tag{4.17}$$

Depending on the previous equations (4.14-4.16), we reformulate (4.17) as

$$\hat{\mathbf{D}}^T = \sum_{l=0}^{NM-1} \left( \mathbf{W}_{d,l} (\mathbf{W}_a)^H \mathbf{H}_l \mathbf{D}^T \mathbf{A}^T \left( \mathbf{Z}_{NM}^H \right)^T \mathbf{E}_{l+1} \mathbf{Z}_{NM}^T \left( \mathbf{A}^H \right)^T \right) + \sum_{l=0}^{NM-1} \left( \mathbf{W}_{d,l} (\mathbf{W}_a)^H \mathbf{N} \mathbf{E}_{l+1} \mathbf{Z}_{NM}^T \left( \mathbf{A}^H \right)^T \right) \tag{4.18}$$

where $\mathbf{A}^H$ corresponds to the matched filter GFDM equalizer.

Since we are using ZF, then $\mathbf{W}_{d,l} (\mathbf{W}_a)^H \mathbf{H}_l = \mathbf{I}$, and since $\sum_{l=0}^{NM-1} \mathbf{E}_{l+1} = \mathbf{I}$ we can simplify (4.18) as:

$$\mathbf{Y}_d = \mathbf{D}^T \mathbf{A}^T \mathbf{A}^H + \hat{\mathbf{N}} \mathbf{A}^H \tag{4.19}$$

where $\hat{\mathbf{N}} = \sum_{l=0}^{NM-1} \mathbf{W}_{d,l} \mathbf{W}_a^H N \mathbf{E}_{l+1} \mathbf{Z}_{NM}^T$ is the noise.

### 4.1.3 Hybrid analog-digital equalizer

We propose in this section a two-step equalizer, we first start with the analog part then the digital part is applied. The analog equalizer is computed to minimize the error between hybrid and full digital schemes, then the digital part is computed to remove the interference ignored on the analog part.

For the analog part, the equalizer elements are selected from a dictionary based on the channel array response vectors. The selection procedure considers as a metric the weighted error between the hybrid and the full digital equalizer matrices. Due to hardware constraints, we assume that the analog equalizer is constant over the subcarriers. Then, the digital part is computed on a per subcarrier basis, over the effective channel, to remove the interference ignored on the analog part.

*Optimization Problem*

In this part, a decoupled transmitter-receiver design is assumed for formulating the optimization problem and computing the equalizer matrices.

We can express the optimization problem for a hybrid receiver

$$\begin{aligned}&\left(\mathbf{W}_a, \mathbf{W}_{d,l}\right) = \arg\min \text{BER} \\ &s.\text{t.} \sum_{l=0}^{NM-1} \text{diag}(\mathbf{W}_{d,l}(\mathbf{W}_a)^H \mathbf{H}_l) = NM\mathbf{I}_U \\ &\mathbf{W}_a \in \mathcal{W}_a \ ,\end{aligned} \tag{4.20}$$

taking in consideration that $\mathcal{W}_a$ implies a set of analog coefficients.
To compute the analog part we assume a Maximal Ratio Combining (MRC) at the digital part. Adopting a MRC approach for the digital equalizer, we can simplify (4.20) to

$$\begin{aligned}&\mathbf{W}_a = \arg\min \sum_{l=0}^{NM-1} \left\| \mathbf{W}_{d,l}(\mathbf{W}_a)^H - \mathbf{H}_l^H \right\|_F^2 \\ &s.\text{t.} \sum_{l=0}^{NM-1} \text{diag}(\mathbf{W}_{d,l}(\mathbf{W}_a)^H \mathbf{H}_l) = NM\mathbf{I}_U \\ &\mathbf{W}_a \in \mathcal{W}_a \ ,\end{aligned} \tag{4.21}$$

The solution of the previous equation gives us the analog equalizer matrix.

*The Analog Part*

Due to hardware constraints, the analog equalizer is constant over the subcarriers, the multi user interference is neglected and only the power of intended users is maximized, and as we mentioned in the optimization problem (4.21), an MRC based approach is implemented.
Let $\mathbf{w}_{a,r} \in \mathbb{C}^{N_{rx}}$ be the equalizer vector of the $p$th RF chain such that $\mathbf{W}_{a,p} = [\mathbf{w}_{a,1}, \ldots, \mathbf{w}_{a,p}] \in \mathbb{C}^{N_{rx} \times p}$, and define $\mathbf{W}_{ad,l,p} = \mathbf{W}_{d,l,p}\mathbf{W}_{a,p}^H$, with $\mathbf{W}_{d,l,p} = [\mathbf{w}_{d,l,1}, \ldots, \mathbf{w}_{d,l,p}] \in \mathbb{C}^{U \times p}$, where $\mathbf{w}_{d,l,p} \in \mathbb{C}^U$ . Since $\mathbf{W}_{d,l,p} = [\mathbf{W}_{d,l,p-1}, \mathbf{w}_{d,l,p}]$ and $\mathbf{W}_{a,p} = [\mathbf{W}_{a,p-1}, \mathbf{w}_{a,p}]$ , the hybrid equalizer at the $p$th step is given by

$$\mathbf{W}_{ad,l,p} = \mathbf{W}_{ad,l,p-1} + \mathbf{w}_{d,l,p}\mathbf{w}_{a,p}^H, \ p = 1, ..., N_{rx}^{RF}. \tag{4.22}$$

considering $\mathbf{W}_{res,l,p} = \mathbf{\Omega}_d \bar{\mathbf{W}}_{d,l,p} \mathbf{W}_{a,p}^H \mathbb{E}[\mathbf{y}_l \mathbf{y}_l^H] - \mathbf{\Omega}_d \mathbf{H}_l^H$, and from (4.22) we can rewrite the problem (4.21) as

$$\begin{aligned}&\mathbf{w}_{a,p} = \arg\min \sum_{l=0}^{NM-1} \left\| \mathbf{w}_{d,l,p}\mathbf{w}_{a,p}^H - \mathbf{W}_{res,l,p-1} \right\|_F^2 \\ &\text{s.t. } \mathbf{w}_{a,p} \in \mathcal{F}_{a,p} \,,\end{aligned} \tag{4.23}$$

where $\mathcal{F}_{a,p}$, denotes the set of feasible analog vectors for step $p$.

The optimization problem (4.23) simplifies to

$$n_{opt,p} = \arg\max_{r=1,\ldots,N_{cl}N_{ray}U} \sum_{l=0}^{NM-1} \left[\mathbf{A}_{rx}^{H}\mathbf{W}_{res,l,p-1}^{H}\mathbf{W}_{res,l,p-1}\mathbf{A}_{rx}\right]_{r,r}, \tag{4.24}$$

concidering $\mathbf{A}_{rx} = [\mathbf{A}_{rx,1}, \ldots, \mathbf{A}_{rx,U}] \in \mathbb{C}^{N_{rx}\times N_{cl}N_{ray}U}$, and $\mathbf{A}_{rx,u} = \left[\mathbf{a}_{rx,u}\left(\phi_1^u - \varphi_{1,1}^u\right), ..., \mathbf{a}_{rx,u}\left(\phi_{N_{cl}}^u - \varphi_{N_{cl},N_{ray}}^u\right)\right]$. where $\mathbf{w}_{a,p} = \mathbf{A}_{rx}^{(n_{opt,p})}$.
For the mentioned purpose, an equalization algorithm is presented in figure 4.3 according to [74].

**Algorithm 1: Analog equalizer**

1: $\mathbf{W}_{a,0}$ = **Empty Matrix**

2: $\mathbf{W}_{res,l,0} = \mathbf{H}_l^H$

3: **for** $p = 1, \ldots, N_{rx}^{RF}$ **do**

4: $n_{opt,p} = \arg\max_{r=1,\ldots,N_{cl}N_{ray}U} \sum_{l=0}^{NM-1} \left[\mathbf{A}_{rx}^{H}\mathbf{W}_{res,l,p-1}^{H}\mathbf{W}_{res,l,p-1}\mathbf{A}_{rx}\right]_{r,r}$

5: $\mathbf{W}_{a,p} = [\mathbf{W}_{a,p-1} \mid \mathbf{A}_{rx}^{(n_{opt,p})}]$

6: To compute $\bar{\mathbf{W}}_{d,l,p}\left[\mathbf{W}_{a,p}\right]$ using (4.11)

7: $\mathbf{\Omega}_p = NM\text{diag}\left(\sum_{l=0}^{NM-1}\left[\bar{\mathbf{W}}_{d,l,p}(\mathbf{W}_{a,p})^H\mathbf{H}_l\right]\right)^{-1}$

8: $\mathbf{W}_{res,l,p} = \mathbf{\Omega}_d\bar{\mathbf{W}}_{d,l}(\mathbf{W}_a)^H\mathbb{E}[\mathbf{y}_l\mathbf{y}_l^H] - \mathbf{\Omega}_d\mathbf{H}_l^H$

9: **end for**

10: **return** $\mathbf{W}_a = \mathbf{W}_{a,N_{rx}^{RF}}$

**Figure 4.3:** The proposed analog equalizer algorithm

In the proposed algorithm, first we initialized the analog and residue matrices, then there is a loop where the work is performed by selecting one equalizer vector of $N_{rx}^{RF}$ each time, i.e., we set a loop where in each iteration we select a vector until the total of $N_{rx}^{RF}$.
In the loop, first the vector is selected considering the criteria of line 4, which we add to our set of selected vectors in line 5. After that, a temporary digital matrix is computed as illustrated in line 6, and from the equation in line 7 we can get the normalization constant. Finally, residue matrix is updated at the end of each loop as shown in line 8.

*The Digital Part*

At the end the digital part is performed, the main goal is to cancel the neglected interference in the analog part to avoid the complex computation inherent to the use of high-dimension matrices. Therefore, assuming a ZF receiver, in order to remove the interference which was neglected in the analog part.
We assume that the digital equalizer is given by

$$\bar{\mathbf{W}}_{d,l} = \left(\mathbf{H}_{eq,l}^{H}\mathbf{H}_{eq,l}\right)^{-1}\mathbf{H}_{eq,l}^{H} \tag{4.25}$$

where $\mathbf{H}_{eq,l} = (\mathbf{W}_a)^H\mathbf{H}_l$ denotes the equivalent channel with the analog equalizer matrix included.

## 4.2 PERFORMANCE RESULTS

The main performance results of the proposed hybrid analog-digital multiuser equalizer, designed for GFDM based systems, are shown in this Section. The results are presented in terms of Bit Error Rate (BER) as a function of the average $E_b/N_0$ . The Quadrature Phase Shift Keying (QPSK) is the modulation scheme adopted in this Section. The table 4.1 presents the parameters of the simulation of the proposed work.

**Table 4.1:** Simulation Parameters

| Parameters | Variables | Value |
|---|---|---|
| Modulation type | - | GFDM |
| Modulation sheme | $\mu$ | QPSK |
| Samples per symbol | $N$ | 64 |
| Number of subcarriers | $K$ | 64 |
| Number of timeslots | $M$ | 15 |
| Duration of time-slot | - | $256\mu s$ |
| Subcarrier bandwidth | - | $3.906KHz$ |
| Oversampling factor | $L$ | 1 |
| Filter type | - | RRC |
| Roll-off factor | $\alpha$ | 0.5 |
| Number of users | $U$ | 4 |
| Transmitting antennas | $N_{tx}$ | 8 or 16 |
| Receiving antennas | $N_{rx}$ | 32 or 64 |

The proposed scheme are evaluated under mmWave WB channel condition, with the parameters presented in the following table

**Table 4.2:** Channel Parameters

| Parameters | Value |
|---|---|
| Array configuration | ULA |
| Time in samples where the channel rays has a significant power | $D = NM/4 = 240$ |
| Carrier frequency | $f_c = 72\,\text{GHz}$ |
| Antenna element spacing | $\delta = \lambda/2$ |
| Number of clusters | $N_{cl} = 4$ |
| Number of rays per cluster | $N_{ray} = 5$ |
| Decay from the first to the last channel cluster | $\beta_{0,N_{cl}-1} = 10\,\text{dB}$ |
| Decay from the first to the last ray of each channel cluster | $\beta_{q,0,N_{ray}-1} = 10$,dB,$q = 0, ..., N_{cl} - 1$ |

According to the previous 4.1 and 4.2 tables , GFDM system is implemented using QPSK modulation for number of sub carriers $K = 64$ and block size $M = 15$. The number of samples per symbol is equal to the number of sub carriers $N = K = 64$.

1. *System performance for* $N_{tx} = 8$, $N_{rx} = 32$

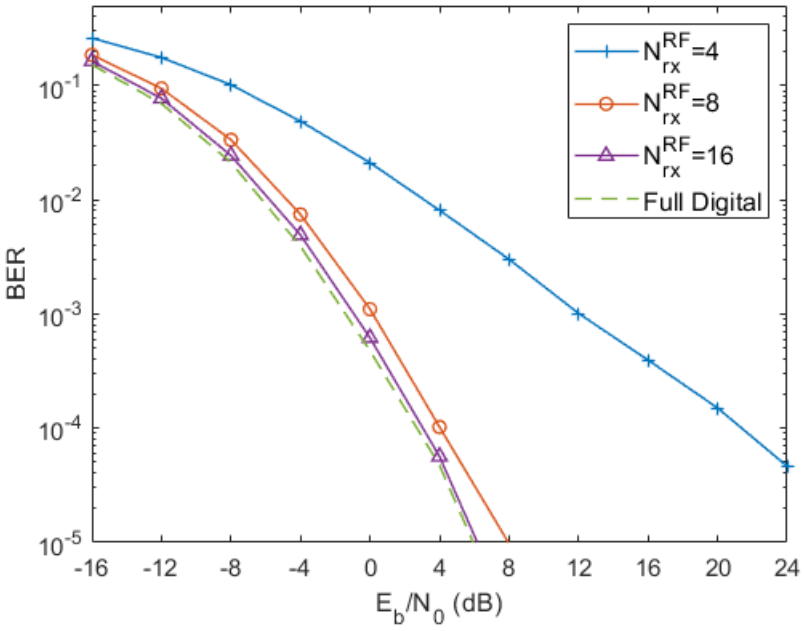


**Figure 4.4:** Performance comparison between the proposed Random based hybrid precoder and the full digital system for $N_{tx} = 8$, $N_{rx} = 32$

This figure 4.4 represents the results for the discussed work, taking into consideration that the number of the transmitting antennas is $N_{tx} = 8$ , and the number of the receiving antennas is $N_{rx} = 32$ for different number of RF chains, where $N_{rx}^{RF} = 4,\ 8,\ 16,\ 32$. We

can notice the obvious logical results, where the performance improves for both cases as the number of RF chains increases, as expected. The best performance among the addressed hybrid cases was when $N_{rx}^{RF} = 16$, with a gap only around 0.5 dB at BER target of $10^{-3}$ compared to the full digital curve where the number of RF chains is 32. Hence, we can say that with this new hybrid scheme, we could obtain almost the same results compared to full digital ones but with the half or less numbers of the RF chains. Where we can also observe that the performance of the system with $N_{rx}^{RF} = 8$ is very close to the performance of the system with $N_{rx}^{RF} = 16$ , with a notable progress from the curve of $N_{rx}^{RF} = 4$ especially at high SNR region.

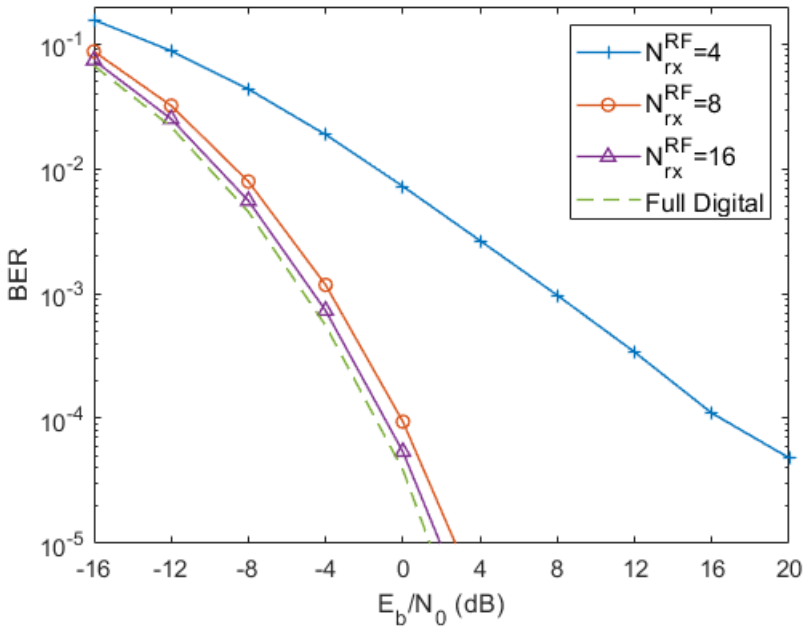


**Figure 4.5:** Performance comparison between the proposed AoD based hybrid precoder and the full digital system for $N_{tx} = 8$, $N_{rx} = 32$

Here figure 4.5 presents different case, it compares the performance of the same parameters but with the use of partial CSI at the transmitter side, which helps to obtain more accurate and reliable results. The attitude in general is similar to the previous case where the best one among the hybrid cases is when $N_{rx}^{RF} = 16$ , with a very close results to the full digital case, but less complicated. All the curves in figure 4.5 show better attitude due to the use of AoD based precoder compared to the previous results where there was no CSI in formations at the transmitter side.

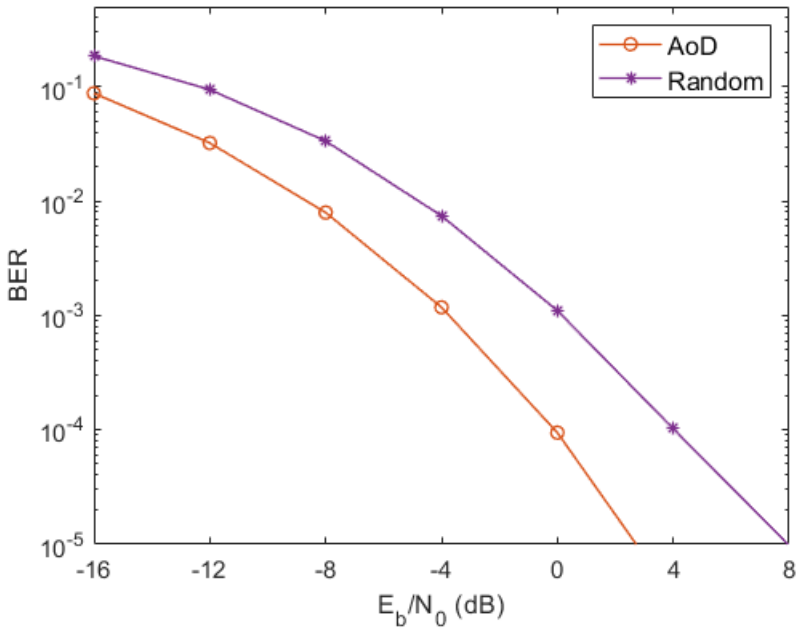


**Figure 4.6:** Performance comparison between the proposed hybrid AoD and Random based precoders for $N_{tx} = 8$, $N_{rx} = 32$, $N_{rx}^{RF} = 8$

This figure 4.6 verifies the idea, it clearly presents the enhancement in the performance of the two discussed cases, for $N_{rx}^{RF} = 8$ , where the case of partial CSI gives better results with around 4 dB increase at BER $= 10^{-3}$ compared to the random precoding approach which is expected since the information about the channels at the terminals is quite small. i.e., with only the knowledge of average AoD information at the UT with the proposed efficient hybrid equalizers, the average BER performance has a significant improvement.

2. *System performance for* $N_{tx} = 16$, $N_{rx} = 64$

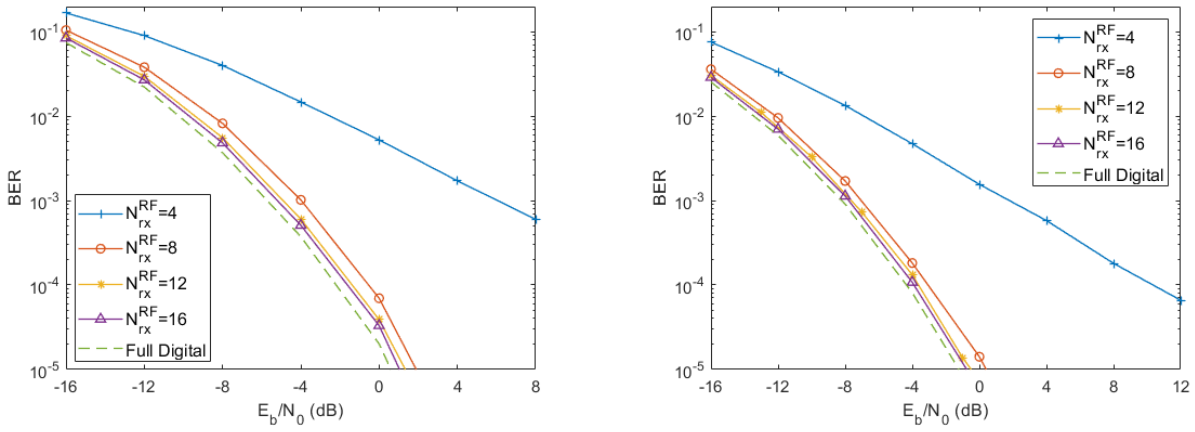


**(a)** Random based precoder **(b)** AoD based precoder

**Figure 4.7:** Performance comparison between the proposed hybrid precoder and the full digital system for $N_{tx} = 16$, $N_{rx} = 64$

Even with the increasing number of transmitting and receiving antennas, we can obtain the same conclusion for both cases, the performance tends to the one obtained with full digital approach when the number of RF chains increases as expected. The diversity order increases the performance toward the full digital curve. Nevertheless, the AoD based precoder (case b) clarifies the enhancement of the system performance, i.e., the slope will be increased due to the diversity gain more than in the first case (a).

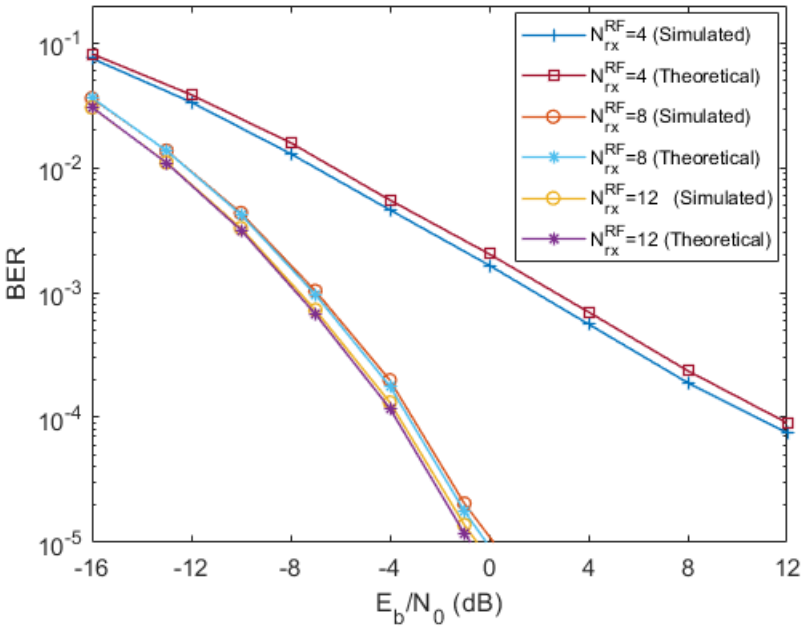


**Figure 4.8:** Performance comparison for the proposed hybrid AoD based precoder between theoretical and simulation cases for$N_{tx} = 16$, $N_{rx} = 64$

We compare the simulation results with the semi analytic BER approximation. The theoretical curves almost overlap with the simulation curves in the case of 8 RF chains. But applying the same conditions on the same scheme with 4 RF chains, the simulation and theoretical curves only overlap at high SNR region. Therefore, we conclude that the higher number of RF chains, the better BER performance due to the diversity that occurs which in turn leads to better and more reliable results, and the case of 12 RF chains verify the conclusion.

3. *Applying Shadowing effect to the channel*

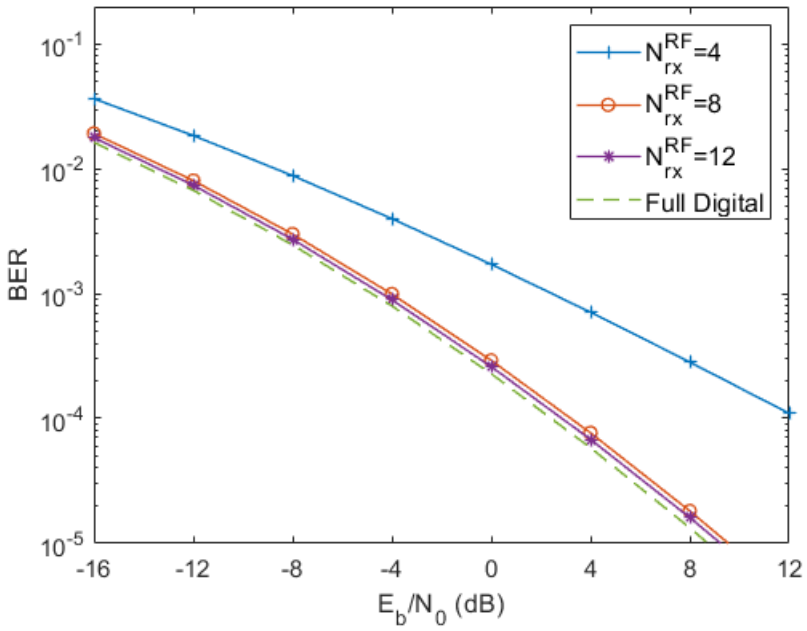


**Figure 4.9:** Performance comparison between the proposed hybrid AoD based precoder after applying shadowing effect.

This figure 4.9 is to illustrate the shadowing effect with path-loss exponent $n_p = 4.17$ and shadowing standard deviation with the value 9 dB. the impact of the path loss and the shadowing effects is evaluated. As we can see, the BER performance improves as the number of RF chains increase, as we saw for scenarios without path loss and shadowing effects. Therefore, we can draw approximately the same conclusions that we obtained before.

CHAPTER 5

# Conclusion and Future Work

*Due to the exponential increase in the demands of exploiting the cellular network resources, to achieve higher data rates and capacity, raised by the smart devices and multimedia applications of new generations, existing cellular networks are facing significant burden. To provide a solution to the challenges faced by 5G networks, there is an utmost need for improving existing technologies as well as developing new technologies to meet the key requirements of beyond 5G networks and the Next Generation Mobile Networks. Moreover, both mmWave communications and mMIMO are key enabling elements for future wireless communication, and has been the destination of many researchers in order to meet the requirements as they are considered a promising approach to achieve the multi Gb/s required by future wireless systems. Therefore, this study focuses on a new approach of implementing signal processing technique (precoding and equalization) for future cellular systems in combination with mmWave and mMIMO concepts.*

## 5.1 CONCLUSION

This work is based on the implementation of a low complexity design for GFDM transceiver, which is a filtered multi-carrier approach that can offer an increased flexibility able to exploit the sparse representation of the sub-carrier filter in frequency domain. The work presented the principles of GFDM where it basically depends on the modulation of independent blocks. Each block consists of a number of sub carriers and sub symbols, to enable the allocation of the fragmented spectrum and the dynamic spectrum without severe interference in incumbent services or other users. The performance of GFDM was analyzed in a new proposed full-connected hybrid system, in which the number of RF chains is lower than the number of antennas. Since this work was designed for WB mmWave channel, it's harder to send and detect WB signals, as the energy of the signal is distributed across the width of the spectrum which makes the signal weaker the wider it gets (transmitting on a given power level). Thus, we used a low-complexity analog precoders to be employed at each UT(transmitter side) that is based on partial knowledge of CSI. The proposed system has two main parts at both

the transmitter and the receiver sides, the digital part is where the GFDM modulation is performed, while the analog part is mainly a proposed analog equalizer based on minimizing the mean square error between the hybrid approach and the full digital counterpart. For this purpose, new algorithm was developed, achieving interesting results that showed the efficiency of the proposed equalizer in removing the multiuser interference;

- The results distinctly illustrated the satisfying performance; the outcomes of the hybrid schemes were close to the digital counterparts with around 70% less RF chains. These results emphasize the main purpose of this work which is less complexity for almost the same performance.
- GFDM is a flexible multi-carrier transmission technique. It allows controlling the out-of-band emissions and the PAPR, which are the major drawbacks of OFDM technology.
- Substantially, the proposed hybrid receiver structures combined with the low complexity analog precoder are attractive to be used in the future systems that are based on mmWave mMIMO technologies, due to the efficient performance with low cost and complexity.

## 5.2 FUTURE WORK

Applying low complexity as well as low cost hybrid architecture on GFDM modulation technique, addresses new features and challenges on the future of telecommunication systems. Some of the following points could be useful suggestions:

1. It can be possible to implement the schemes with higher-order constellations (e.g. 16/64/256-QAM) already considered in 5G and comparing with the results of QPSK used.
2. In general, CSI acquisition for mMIMO systems is a challenging task due to the presence of noise and the estimation errors caused by the unpredictability of the frequency division duplex (FDD) mode. Investigating the performance of the proposed hybrid beamforming algorithms when channel estimation errors are introduced is the first step towards extending this research.
3. Another way can be used is by grouping the users into clusters according to their location, the RF beamformer can increase the SNR of the users in each cluster. Then, base-band precoder can mitigate the interference between the users in each cluster by using accurate CSI of the effective channel.
4. The proposed equalizer can also be extended, it can be implemented with other hybrid architectures such as sub-connected where the needed RF chains is less, and thus the complexity can be reduced.

# References


[1] A. Ericsson, *Gsm system survey*, 2008.

[2] H. Mehta, D. Patel, B. Joshi, and H. Modi, "0g to 5g mobile technology: A survey", *J. of Basic and Applied Engineering Research*, vol. 1, no. 6, pp. 56–60, 2014.

[3] M. R. Bhalla and A. V. Bhalla, "Generations of mobile wireless technology: A survey", *International Journal of Computer Applications*, vol. 5, no. 4, pp. 26–32, 2010.

[4] M. A. Albreem, "5g wireless communication systems: Vision and challenges", in *2015 International Conference on Computer, Communications, and Control Technology (I4CT)*, IEEE, 2015, pp. 493–497.

[5] Y. Park and F. Adachi, *Enhanced radio access technologies for next generation mobile communication*. Springer, 2007.

[6] A. Kukushkin, *Introduction to Mobile Network Engineering: GSM, 3G-WCDMA, LTE and the Road to 5G*. John Wiley & Sons, 2018.

[7] A. Mohammed Sb, "The principle of ofdm and use in 4g radio cellular systems", *International Journal of Computer Applications*, vol. 182 – No. 27, pp. 46–49, Nov. 2018. DOI: 10.5120/ijca2018918127.

[8] L. J. Vora, "Evolution of mobile generation technology: 1g to 5g and review of upcoming wireless technology 5g", *International journal of modern trends in engineering and research*, vol. 2, no. 10, pp. 281–290, 2015.

[9] A. L. Swindlehurst, E. Ayanoglu, P. Heydari, and F. Capolino, "Millimeter-wave massive mimo: The next wireless revolution?", *IEEE Communications Magazine*, vol. 52, no. 9, pp. 56–62, 2014.

[10] M. R. Akdeniz, Y. Liu, S. Rangan, and E. Erkip, "Millimeter wave picocellular system evaluation for urban deployments", in *2013 IEEE Globecom Workshops (GC Wkshps)*, IEEE, 2013, pp. 105–110.

[11] W. Roh, J.-Y. Seol, J. Park, B. Lee, J. Lee, Y. Kim, J. Cho, K. Cheun, and F. Aryanfar, "Millimeter-wave beamforming as an enabling technology for 5g cellular communications: Theoretical feasibility and prototype results", *IEEE communications magazine*, vol. 52, no. 2, pp. 106–113, 2014.

[12] A. Alkhateeb, J. Mo, N. Gonzalez-Prelcic, and R. W. Heath, "Mimo precoding and combining solutions for millimeter-wave systems", *IEEE Communications Magazine*, vol. 52, no. 12, pp. 122–131, 2014.

[13] S. Han, I. Chih-Lin, Z. Xu, and C. Rowell, "Large-scale antenna systems with hybrid analog and digital beamforming for millimeter wave 5g", *IEEE Communications Magazine*, vol. 53, no. 1, pp. 186–194, 2015.

[14] A. Grami, *Introduction to Digital Communications*. Academic Press, 2015.

[15] H. A. AL-Khafaji and H. M. AlSabbagh, "Simple analysis of ber performance for bpsk and mqam over fading channel", *International Journal of Computing and Digital Systems*, vol. 6, no. 05, pp. 303–310, 2017.

[16] R. Chisab, "42101-7474-ijet-ijens © february 2014 ijens", *ijens*, vol. 14, pp. 1–58, Jan. 2014.

[17] W. C. Jakes and D. C. Cox, *Microwave mobile communications*. Wiley-IEEE Press, 1994.

[18] J. D. Parsons, *The mobile radio propagation channel*. Wiley, 2000.

[19] R. Legnain, "Smart antennas for cellular mobile systems", PhD thesis, Jul. 2004. DOI: 10.13140/RG.2.1.2272.6008.

[20] A. Goldsmith, *Wireless communications*. Cambridge university press, 2005.

[21] Y.-C. Ko, "Doppler spread estimation in mobile communication systems", *IEICE transactions on communications*, vol. 88, no. 2, pp. 724–728, 2005.

[22] B. Sklar, "Rayleigh fading channels in mobile digital communication systems. i. characterization", *IEEE Communications magazine*, vol. 35, no. 7, pp. 90–100, 1997.

[23] J. K. Tugnait, "Channel estimation, equalization, precoding, and tracking", in *Academic Press Library in Signal Processing*, vol. 2, Elsevier, 2014, pp. 95–133.

[24] P. JG, "Digital communications", *Me Graw-Hill*, pp. 777–778, 2001.

[25] J. Yang, E. Mostafapour, A. Aminfar, J. Wang, H. Huang, A. Akhbari, C. Ghobadi, and G. Gui, "Channel fading effect analysis on diffusion cooperation strategies over adaptive networks", *KSII Transactions on Internet and Information Systems*, vol. 13, pp. 172–185, Jan. 2019. DOI: 10.3837/tiis.2019.01.010.

[26] M. Viswanathan, "Simulation of digital communication systems using matlab", *Mathuranathan Viswanathan at Smashwords*, 2013.

[27] Y. Miyake, K. Kobayashi, K. Komatsu, S. Tanifuji, H. Oguma, N. Izuka, S. Kameda, N. Suematsu, T. Takagi, and K. Tsubouchi, "Hybrid single-carrier and multi-carrier system: Widening uplink coverage with optimally selecting sdm or join fde/antenna diversity", in *2011 The 14th International Symposium on Wireless Personal Multimedia Communications (WPMC)*, IEEE, 2011, pp. 1–5.

[28] D. P. Maxson, *The IBOC Handbook: Understanding HD Radio (TM) Technology*. CRC Press, 2007.

[29] M. Rumney *et al.*, *LTE and the evolution to 4G wireless: Design and measurement challenges*. John Wiley & Sons, 2013.

[30] G. Prashanth, "Orthogonal frequency division multiplexing (ofdm) based uplink multiple access method over awgn and fading channels", 2019.

[31] H. Nourollahi and S. G. Maghrebi, "Evaluation of cyclic prefix length in ofdm system based for rayleigh fading channels under different modulation schemes", in *2017 IEEE Symposium on Computers and Communications (ISCC)*, IEEE, 2017, pp. 164–169.

[32] M. Sameen, A. A. Khan, I. U. Khan, N. Azim, I. Shafi, T. Zaidi, and N. Iqbal, "Comparative analysis of ofdm and gfdm", *International Journal of Advance Computing Techniques and Applications*, 2016.

[33] K. Fazel and S. Kaiser, *Multi-carrier and spread spectrum systems: from OFDM and MC-CDMA to LTE and WiMAX*. John Wiley & Sons, 2008.

[34] N. Michailow, M. Matthé, I. S. Gaspar, A. N. Caldevilla, L. L. Mendes, A. Festag, and G. Fettweis, "Generalized frequency division multiplexing for 5th generation cellular networks", *IEEE Transactions on Communications*, vol. 62, no. 9, pp. 3045–3061, 2014.

[35] R. Datta, N. Michailow, M. Lentmaier, and G. Fettweis, "Gfdm interference cancellation for flexible cognitive radio phy design", in *2012 IEEE Vehicular Technology Conference (VTC Fall)*, IEEE, 2012, pp. 1–5.

[36] B. M. Alves, L. L. Mendes, D. A. Guimaraes, and I. S. Gaspar, "Performance of gfdm over frequency-selective channels", in *Proc. Int. Workshop Telecommun*, 2013, pp. 1–7.

[37] R. S. Kshetrimayum, *Fundamentals of MIMO wireless communications*. Cambridge University Press, 2017.

[38] L. Zheng and D. N. C. Tse, "Diversity and multiplexing: A fundamental tradeoff in multiple-antenna channels", *IEEE Transactions on Information Theory*, vol. 49, no. 5, pp. 1073–1096, 2003.

[39] A. Silva and A. Gameiro, *Multiple Antenna Systems*. Aveiro: DETI, University of Aveiro, 2018.

[40] C. R. Shah, *Performance and comparative analysis of siso, simo, miso, mimo*, 2017.

[41] P. Almers, E. Bonek, A. Burr, N. Czink, M. Debbah, V. Degli-Esposti, H. Hofstetter, P. Kysti, D. Laurenson, G. Matz, *et al.*, "Survey of channel and radio propagation models for wireless mimo systems", *EURASIP Journal on Wireless Communications and Networking*, vol. 2007, no. 1, p. 019 070, 2007.

[42] G. Tsoulos, *MIMO system technology for wireless communications*. CRC press, 2006.

[43] R. Mahey and J. Malhotra, "On mimo channel modeling for the mobile wireless systems", *International Journal of Future Generation Communication and Networking. INDIA*, vol. 8, no. 5, pp. 23–38, 2015.

[44] T. Javornik, G. Kandus, S. Plevel, and S. Tomazic, *Mimo: Wireless communications*. 2008.

[45] L. Lu, G. Y. Li, A. L. Swindlehurst, A. Ashikhmin, and R. Zhang, "An overview of massive mimo: Benefits and challenges", *IEEE journal of selected topics in signal processing*, vol. 8, no. 5, pp. 742–758, 2014.

[46] E. G. Larsson, O. Edfors, F. Tufvesson, and T. L. Marzetta, "Massive mimo for next generation wireless systems", *IEEE communications magazine*, vol. 52, no. 2, pp. 186–195, 2014.

[47] H. Q. Ngo, E. G. Larsson, and T. L. Marzetta, "Energy and spectral efficiency of very large multiuser mimo systems", *IEEE Transactions on Communications*, vol. 61, no. 4, pp. 1436–1449, 2013.

[48] E. G. Larsson, "Very large mimo systems: Opportunities and challenges", *Linköping University*, 2012.

[49] C. Studer and E. G. Larsson, "Par-aware large-scale multi-user mimo-ofdm downlink", *IEEE Journal on Selected Areas in Communications*, vol. 31, no. 2, pp. 303–313, 2013.

[50] S. K. Mohammed and E. G. Larsson, "Per-antenna constant envelope precoding for large multi-user mimo systems", *IEEE Transactions on Communications*, vol. 61, no. 3, pp. 1059–1071, 2013.

[51] J. Hoydis, S. Ten Brink, and M. Debbah, "Massive mimo in the ul/dl of cellular networks: How many antennas do we need?", *IEEE Journal on selected Areas in Communications*, vol. 31, no. 2, pp. 160–171, 2013.

[52] D. C. Araújo, T. Maksymyuk, A. L. de Almeida, T. Maciel, J. C. Mota, and M. Jo, "Massive mimo: Survey and future research topics", *Iet Communications*, vol. 10, no. 15, pp. 1938–1946, 2016.

[53] X. Gao, O. Edfors, F. Rusek, and F. Tufvesson, "Linear pre-coding performance in measured very-large mimo channels", in *2011 IEEE Vehicular Technology Conference (VTC Fall)*, IEEE, 2011, pp. 1–5.

[54] S. Akoum, O. El Ayach, and R. W. Heath, "Coverage and capacity in mmwave cellular systems", in *2012 conference record of the forty sixth Asilomar conference on signals, systems and computers (ASILOMAR)*, IEEE, 2012, pp. 688–692.

[55] I. A. Hemadeh, K. Satyanarayana, M. El-Hajjar, and L. Hanzo, "Millimeter-wave communications: Physical channel models, design considerations, antenna constructions, and link-budget", *IEEE Communications Surveys & Tutorials*, vol. 20, no. 2, pp. 870–913, 2017.

[56] C. Anioke, C. Nnamani, and C. Ani, "Review of wireless mimo channel models", *Nigerian Journal of Technology*, vol. 35, no. 2, pp. 381–391, 2016.

[57] D. Pant, A. Gupta, S. Singh, and S. Sachan, "Mimo channel modelling methods: An overview", Jan. 2013.

[58] A. Meijerink and A. F. Molisch, "On the physical interpretation of the saleh–valenzuela model and the definition of its power delay profiles", *IEEE transactions on antennas and propagation*, vol. 62, no. 9, pp. 4780–4793, 2014.

[59] F. Grejták and A. Prokes, "Uwb-ultra wideband characteristics and the saleh-valenzuela modeling", *Acta Electrotechnica et Informatica*, vol. 13, no. 2, p. 32, 2013.

[60] N. O. Oyie and T. J. Afullo, "Spatiotemporal statistical channel model for indoor corridor at 14 ghz, 18 ghz, and 22 ghz bands", *Wireless Communications and Mobile Computing*, vol. 2018, 2018.

[61] A. Alkhateeb and R. W. Heath, "Frequency selective hybrid precoding for limited feedback millimeter wave systems", *IEEE Transactions on Communications*, vol. 64, no. 5, pp. 1801–1818, 2016.

[62] S. Mumtaz, J. Rodriguez, and L. Dai, *MmWave Massive MIMO: A Paradigm for 5G*. Academic Press, 2016.

[63] V. Venkateswaran and A.-J. van der Veen, "Analog beamforming in mimo communications with phase shift networks and online channel estimation", *IEEE Transactions on Signal Processing*, vol. 58, no. 8, pp. 4131–4143, 2010.

[64] O. El Ayach, S. Rajagopal, S. Abu-Surra, Z. Pi, and R. W. Heath, "Spatially sparse precoding in millimeter wave mimo systems", *IEEE transactions on wireless communications*, vol. 13, no. 3, pp. 1499–1513, 2014.

[65] I. Ahmed, H. Khammari, A. Shahid, A. Musa, K. S. Kim, E. De Poorter, and I. Moerman, "A survey on hybrid beamforming techniques in 5g: Architecture and system model perspectives", *IEEE Communications Surveys & Tutorials*, vol. 20, no. 4, pp. 3060–3097, 2018.

[66] N. Michailow, I. Gaspar, S. Krone, M. Lentmaier, and G. Fettweis, "Generalized frequency division multiplexing: Analysis of an alternative multi-carrier technique for next generation cellular systems", in *2012 International Symposium on Wireless Communication Systems (ISWCS)*, IEEE, 2012, pp. 171–175.

[67] C. H. Doan, S. Emami, D. A. Sobel, A. M. Niknejad, and R. W. Brodersen, "Design considerations for 60 ghz cmos radios", *IEEE Communications Magazine*, vol. 42, no. 12, pp. 132–140, 2004.

[68] Z. Pi and F. Khan, "An introduction to millimeter-wave mobile broadband systems", *IEEE communications magazine*, vol. 49, no. 6, pp. 101–107, 2011.

[69] A. Valdes-Garcia, S. T. Nicolson, J.-W. Lai, A. Natarajan, P.-Y. Chen, S. K. Reynolds, J.-H. C. Zhan, D. G. Kam, D. Liu, and B. Floyd, "A fully integrated 16-element phased-array transmitter in sige bicmos for 60-ghz communications", *IEEE journal of solid-state circuits*, vol. 45, no. 12, pp. 2757–2773, 2010.

[70] C. Cox, *An introduction to LTE: LTE, LTE-advanced, SAE and 4G mobile communications*. John Wiley & Sons, 2012.

[71] M. Jankiraman, *Space-time codes and MIMO systems*. Artech House, 2004.

[72] R. Magueta, D. Castanheira, A. Silva, R. Dinis, and A. Gameiro, "Two-step analog-digital multiuser equalizer for hybrid precoded mmwave communications", in *2018 IEEE Globecom Workshops (GC Wkshps)*, IEEE, 2018, pp. 1–6.

[73] I. Gaspar, N. Michailow, A. Navarro, E. Ohlmer, S. Krone, and G. Fettweis, "Low complexity gfdm receiver based on sparse frequency domain processing", in *2013 IEEE 77th Vehicular Technology Conference (VTC Spring)*, IEEE, 2013, pp. 1–6.

[74] R. Magueta, D. Castanheira, P. Pedrosa, A. Silva, R. Dinis, and A. Gameiro, "Iterative analog–digital multi-user equalizer for wideband millimeter wave massive mimo systems", *Sensors*, vol. 20, no. 2, p. 575, 2020.